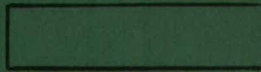


LWL
CR-05P70
c.1



20080924 284

Technical Memorandum NO. LWL-CR-05P70

EFFECT OF A FOREST ENVIRONMENT
ON THE PERFORMANCE OF DOPPLER RADAR SYSTEMS

Interim Report

TECHNICAL LIBRARY

BLDG. 305

By **ABERDEEN PROVING GROUND, MD.**
STEAP-TL

T. Tamir; Ph.D.
Consultant

COUNTED IN

Prepared Under
Contract DA-31-124-AROD-120

December 1971

Approved for public release; distribution unlimited

U. S. ARMY LAND WARFARE LABORATORY
Aberdeen Proving Ground, Maryland 21005

LWL
CR-05P70
c.1



AD-741349

Technical Memorandum No. LWL-CR-05P70

EFFECT OF A FOREST ENVIRONMENT
ON THE PERFORMANCE OF DOPPLER RADAR SYSTEMS

Interim Report

By

T. Tamir, Ph. D.
Consultant

Prepared Under
Contract DA-31-124-AROD-120

December 1971

Approved for public release; distribution unlimited

U.S. Army Land Warfare Laboratory
Aberdeen Proving Ground, Maryland 21005

TECHNICAL LIBRARY
BLDG. 305
ABERDEEN PROVING GROUND, MD.
STEAP-TL

ABSTRACT

The aim of this report is to examine the effect of a forest environment on the performance of a remote sensing system that detects the Doppler-shifted signal scattered by moving objects. For this purpose, the influence of the terrain on the radar equation is determined by estimating the additional path loss due to the presence of dissipative media between the transmitter antenna and the moving scatterer. For most situations of practical importance, it is shown that the additional path loss can be expressed in terms of a terrain factor, which accounts for the presence of both the foliage and the ground. This terrain loss is evaluated for the case of a moving target located in the vegetation, and for a transmitter antenna that may be placed either inside the vegetation or above the tree tops. The calculated results are given for a wide range of distances between the antenna and the target, for various antenna heights and for different types of wooded areas.

ACKNOWLEDGEMENT

This report was prepared to assist the Land Warfare Laboratory in developing performance criteria for a VHF foliage penetration radar system. The assistance provided by the LWL Task Officer, Mr. Louis V. Surgent, Jr., in defining the radar problem and in obtaining data for this analysis is greatly appreciated. The encouragement and valuable discussions provided by Mr. Jacob Wenig, Chief, Applied Physics Branch are gratefully acknowledged.

TABLE OF CONTENTS

	ABSTRACT	
I.	INTRODUCTION	1
II.	GENERAL CONSIDERATIONS	3
III.	DEFINITION OF TERRAIN LOSS	5
IV.	DERIVATION OF TERRAIN LOSS	9
	A. Antenna Within the Vegetation Layer	10
	B. Antenna Above Tree Tops	14
V.	TERRAIN LOSS CALCULATIONS	17
	A. Classification of Forest Parameters	17
	B. Antenna Within Vegetation Layer	18
	C. Antenna Above Vegetation Layer	19
	D. Antenna Height Gain	21
	E. Variation of L_t with the Range ρ	22
VI.	VEGETATION LOSS CALCULATIONS	23
VII.	CONCLUSIONS	25
	References	27
	List of Figures	28
	Figures	30

I. INTRODUCTION

A remote sensing system usually consists of a transmitter that beams electromagnetic energy onto a selected region of space. Because objects located within this illuminated region generally scatter energy in all directions, it is possible to locate and identify them by selectively detecting a portion of the scattered energy. Usually, both the transmitter and the receiver form part of a single unit, which utilizes the same antenna both for transmitting the signal and for receiving the back scattered response. Although the results in the present report do not require that this be the case, it will be assumed for simplicity that a single antenna serves both the receiving and transmitting functions.

The performance of a remote sensing system may depend strongly on the particular environment where the system actually operates. In particular, the gain and effectiveness of the antenna is affected by the type of terrain that is illuminated by the antenna beam. Furthermore, the path traversed by the electromagnetic energy (from the antenna to the illuminated scatterer and back) has a pronounced effect on the overall sensitivity of the system; thus, this sensitivity is considerably reduced if lossy media intervene. However, the specifications of the system are usually given in terms of a free-space path, which implicitly assumes that the antenna pattern is not affected by the presence of extraneous media in its immediate vicinity. At best, the effect of ground proximity on the antenna pattern may sometimes be specified for various antenna heights, but the effects of any other stationary media in the illuminated region are usually disregarded.

The aim of the present work is to examine and evaluate the effect of vegetation on the operation of a Doppler sensing system when the region illuminated by the antenna occurs partly or entirely within a forest environment. Whereas propagation studies in such environments have already considered the effects of vegetation on the radiated field,^(1, 2) no investigation has been carried out to estimate this effect on the radiation pattern and/or on the

total sensitivity of a system. The principal result of the present study expresses the environmental effects in terms of a quantity that predicts the reduction in the overall sensitivity due to the lossy media which occur along or close to the radio-wave path linking the antenna to a moving scatterer to be detected. This quantity, termed here "terrain loss", represents the difference in decibels between the sensitivity of the system under free-space conditions and the sensitivity under the actual forest-terrain conditions. As derived here, the terrain loss includes the effect on system performance of both the ground proximity and the presence of vegetation. This terrain loss is evaluated over a range of parameters, which cover many situations that occur in a large class of forest environments.

II. GENERAL CONSIDERATIONS

The work described in this report assumes that the scatterer consists of a moving target, which is detected by means of the Doppler frequency that is produced in the scattered signal. In particular, the present study has been undertaken to cover the following ranges of pertinent parameters:

- (a) The target to be detected is a walking man whose body center is taken to be located at a height $z=1$ meter above ground.
- (b) The distance between the transmitter and the target should range from 50 meters to 2 kms.
- (c) The frequency of operation is 140 MHz.
- (d) The transmitting antenna could be placed either inside the vegetation or above the tree tops, at heights that vary from 1 to 30 meters. A typical antenna to be considered is specified with a 35° horizontal and 15° vertical beamwidth in free space; its polarization is horizontal.
- (e) The types of vegetation include thickly wooded areas, forests with moderate amounts of trees and foliage, as well as sparsely covered brush regions.

As described below, all of the above ranges of the various parameters are covered and, in fact, the present work may be used to find the terrain losses for ranges that are wider than those stipulated. Thus, the antenna height may be considerably larger than 30 meters above ground and vertical polarization may also be examined by following the procedure described here. In addition, the present results may be applied to other antennas, as well as to other frequencies in the range of 2 to 200 MHz.

At this stage, it is important to observe that, although the above specifications include a very wide range of values, it is assumed in this report that the target lies in the far field of the antenna. To verify this point, it is recalled that the far field starts roughly at the Fresnel distance

$$r_o = \frac{2A}{\lambda} ,$$

where A is the effective aperture area of the antenna, namely

$$A = \frac{G \lambda^2}{4\pi} .$$

The antenna gain G for the typical antenna mentioned under (d) above is about 50 (= 17 dB). The Fresnel distance for this case is therefore

$$r_o = \frac{G \lambda}{2\pi} = \frac{50 \times 2.15}{2\pi} = 17 \text{ meters.}$$

This distance is well below the minimum detection distance of 50 meters mentioned under (b) above, so that the far field assumption is well justified.

III. DEFINITION OF TERRAIN LOSS

A typical forest environment is sketched in Fig. 1 where, for convenience, the antenna is shown above the tree tops, but its location may lie either inside or above the vegetation layer. To arrive at a quantity that describes the effect of the environment on the system performance, assume that free-space conditions hold between the antenna and the target and consider then the radar equation

$$\frac{P_r}{P_t} = G_t D_t \cdot \sigma \cdot D_r G_r \quad , \quad (1)$$

- where: P_r = R. F. power at the receiver input;
 P_t = R. F. power radiated by the antenna;
 G_t = transmitting antenna gain;
 D_t = reduction in power due to propagation along path between transmitter antenna and target;
 σ = normalized radar cross section of target;
 D_r = reduction in power due to propagation along path between target and receiving antenna;
 G_r = Receiving antenna gain.

Second-order factors, such as those referring to circuit losses, polarization losses, etc., have been assumed negligible and they were therefore omitted in Eq. (1). Because it is assumed that the same antenna serves for both transmitting and receiving functions, one has

$$G_t = G_r = G \text{ and } D_t = D_r = D \quad , \quad (2)$$

so that

$$\frac{P_r}{P_t} = \sigma (GD)^2 \quad (3)$$

Usually, the quantities σ , G and D are specified under free-space conditions. Assume now that σ' , G' and D' denote analogous quantities in the presence of the media shown in Fig. 1. One may then write an equivalent radar equation

$$\frac{P'_r}{P'_t} = \sigma' (G' D')^2, \quad (4)$$

which now holds for the situation shown in Fig. 1 instead of free-space.

When the antenna and/or target are embedded in or close to lossy media, such as vegetation or ground, neither G' nor D' are easily found. In fact, it is not generally possible to individually separate out the factors σ' , G' and D' in a simple manner. In the present case, however, it is possible to obtain a considerable simplification by recalling that the target is detected by means of the Doppler effect. Hence, although the target itself moves in the proximity of other scatterers (such as leaves, trees, etc.), these scatterers are relatively stationary; their back-scattered fields are therefore regarded as background noise and they are rejected by an appropriate integrating circuit in the receiving end of the system. Because of this process, the fields scattered directly by stationary objects tend to cancel out when averaged over the time interval of the integrating circuit. At most, therefore, the stationary scatterers will contribute a detected signal because of secondary scattering of energy that was first scattered by the moving targets. However, this secondary scattering may be neglected since it is expected to possess a magnitude of second-order. Hence, it is reasonable to assume that, to a first-order approximation, the cross section σ' of the target in the presence of stationary scatterers is equal to the cross section σ of the target in the absence of other scatterers, i. e., in free space.

Inserting therefore $\sigma' = \sigma$ in Eq. (3) and dividing thru Eq. (4), one obtains

$$\frac{P_r/P_t}{P'_r/P'_t} = \left(\frac{G}{G'} \frac{D}{D'} \right)^2 \quad (5)$$

The last result serves to define

$$2 L_t = 10 \log \frac{P_r / P_t}{P'_r / P'_t} = 20 \log \frac{G D}{G' D'} \quad (\text{in dB}) \quad , \quad (6)$$

where L_t is the one-way terrain loss. As defined, the product $G D$ denotes the power incident on the target due to one watt of power radiated by the antenna under free-space conditions, whereas $G' R'$ denotes the same quantity under the actual conditions of Fig. 1. Hence, one obtains

$$\begin{aligned} L_t &= 10 \log \frac{G D}{G' D'} \\ &= 10 \log \frac{\text{Incident power (free-space conditions)}}{\text{Incident power (actual conditions)}} \quad . \quad (7) \end{aligned}$$

It is clear that the terrain loss L_t represents the one-way decrease in available power due to terrain conditions. Consequently, L_t may be regarded as a sensitivity reduction that needs to be accounted for in the system if one needs to overcome restrictions that are imposed by a lossy environment. As defined, however, L_t does not include the sensitivity loss due to the operation of the integrating circuit, which is required to eliminate the stationary background clutter.

Although the terrain loss L_t of Eq. (7) is an excellent measure of the effect of the terrain, it is often convenient to distinguish between a terrain consisting of a forest environment and a terrain that involves a bare ground with no vegetation. This is so because the same remote sensing system may sometimes work above bare ground whereas at other times it may be operated in or near vegetation. If one takes G'' and D'' to denote quantities in the presence of bare ground, one obtains

$$\begin{aligned} L_{gr} &= 10 \log \frac{G D}{G'' D''} \\ &= 10 \log \frac{\text{Incident power (free-space conditions)}}{\text{Incident power (bare-ground conditions)}} \quad (8) \end{aligned}$$

where L_{gr} yields the one-way decrease in available power due to the presence of

the ground alone.

By subtracting L_{gr} from L_t , one gets

$$\begin{aligned} L_{veg} &= L_t - L_{gr} = 10 \log \frac{G'' D''}{G' D'} \\ &= 10 \log \frac{\text{Incident power (bare-ground conditions)}}{\text{Incident power (actual conditions)}} , \end{aligned} \quad (9)$$

where L_{veg} yields the one-way sensitivity loss due to vegetation with respect to bare-ground conditions. As defined, L_{veg} represents the sensitivity loss incurred when the remote sensing system is moved from a site containing essentially no vegetation to another site which is covered by a considerable amount of vegetation.

IV. DERIVATION OF TERRAIN LOSS

To derive the terrain loss in a representative forest environment, it is observed that the rather general situation shown in Fig. 1 must be first described in terms of a suitable model. This model is obtained by simplifying both the ground profile and the envelope of the tree canopy and thus arriving at the idealized configuration shown in Fig. 2, wherein the ground plane and the forest-air boundary are assumed to be planar and parallel to each other. The vegetation layer is then assumed to be characterized by a homogeneous lossy medium whose relative permittivity ϵ_1 is complex. Similarly, the ground is characterized by a complex permittivity ϵ_2 .

Although the modelling of the forest environment in terms of the idealized configuration shown in Fig. 2 may seem to be an oversimplification of the actual situation, measurements have indicated that path loss calculations are not considerably affected by a reasonable amount of hilly terrain.⁽³⁾ Also, local variations in the composition of the vegetation are of second-order importance and it is the average height of the trees that determines the effective forest height h .

When calculating the terrain loss L_t for a target inside the forest layer, the location of the antenna is of primary importance because the nature of the electromagnetic field is quite different if the antenna is within the vegetation or outside the forest layer. This is due to the fact that the wave-propagation paths that link the antenna with the target are basically different if the antenna is inside or outside the vegetation layer. The two cases are therefore considered separately and their respective propagation mechanisms are discussed further below.

The modelling shown in Fig. 2 describes the environment only and may therefore be used to evaluate the factor D/D' in Eq. (7); however, the factor G/G' may depend both on the environment and on the particular directive antenna that is used. To account for the second factor, it is necessary to describe the

directive antenna in terms of a canonical form, which is characteristic of a large class of antennas being used at the frequency of interest. Because this frequency is 140 MHz, it is convenient to assume that the antenna consists of a single linear array as shown in Fig. 3. Each element in the array is taken to be a small dipole and a total number of n dipoles is assumed to be present. However, the current I_i in the i^{th} dipole is arbitrary; the inclination and polarization of the entire array with respect to the ground plane may generally also be arbitrary, but the discussion will later be restricted for practical purposes to horizontal arrays with horizontal polarization.

The modelling involved in Fig. 2 (for the environment) and in Fig. 3 (for the directive antenna) makes it possible to derive the terrain loss L_t for a large class of practical situations. This derivation of L_t follows below and the two cases shown in Fig. 2 are examined separately. The results are applicable to situations involving terrains with small amounts of curvature produced by hills, as well as to antennas other than a single dipole array.

A. Antenna Within the Vegetation Layer

If both the transmitting antenna at point T and the target at point R are within the vegetation, the propagation mechanism linking the two terminals is a lateral wave, which follows the segmented path TABR shown in Fig. 4. This lateral-wave propagation has been discussed extensively in the literature;^(1, 2) it is observed that most of the path lies along the segment AB, which means that the lateral wave travels mostly by skimming across the tree tops.

To evaluate the terrain loss L_t , it is convenient to assume that the axis of the array shown in Fig. 3 is located in the xz plane of Fig. 4 and that the center of the array is on the z axis. Let then the origin O' of a cylindrical polar coordinate system coincide with the projection of point R on the xy plane. In that case, the field E_i' produced on the target R at (x, y, z) by a single dipole element located at $(x_i, 0, z_i)$ is given⁽²⁾ by:

1. For vertical polarization (vertical dipoles):

$$E'_{zi} = F_v(z) F_v(z_i) E_{\infty i} \quad (10a)$$

2. For horizontal polarization (horizontal dipoles):

$$E'_{\phi i} = F_h(z) F_h(z_i) E_{\infty i} \cos \phi_i. \quad (10b)$$

Here ϕ_i refers to the azimuth angle between the single dipole and the fields E'_{zi} and $E'_{\phi i}$ denote the electric components of E'_i along the z or the ϕ direction, respectively. These particular directions are chosen because they refer to those field components that are detected by the antenna after the signal is scattered back by the target. The other quantities in Eqs. (8a) and (8b) are given⁽²⁾ by

$$E_{\infty i} = \frac{60 I_i l_i}{\epsilon_1 - 1} \frac{e^{-jk_0 [\rho_i + \sqrt{\epsilon_1 - 1} (2h - z - z_i)]}}{\rho_i^2}, \quad (11)$$

$$F_{v,h} = \frac{1 + \Gamma_{v,h} e^{-2jk_0 \sqrt{\epsilon_1 - 1} z}}{1 - \Gamma_{v,h} e^{-2jk_0 \sqrt{\epsilon_1 - 1} h}} \quad (12)$$

where $k_0 = \omega \sqrt{\mu_0 \epsilon_0}$ is the wavenumber of plane waves in free space and $I_i l_i$ is the dipole moment of the i^{th} element in the array. The reflection coefficients Γ_v and Γ_h refer to vertical and horizontal polarization, respectively, and are given by

$$\Gamma_v = \frac{\epsilon_2 \sqrt{\epsilon_1 - 1} - \epsilon_1 \sqrt{\epsilon_2 - 1}}{\epsilon_2 \sqrt{\epsilon_1 - 1} + \epsilon_1 \sqrt{\epsilon_2 - 1}}, \quad (13a)$$

$$\Gamma_h = \frac{\sqrt{\epsilon_1 - 1} - \sqrt{\epsilon_2 - 1}}{\sqrt{\epsilon_1 - 1} + \sqrt{\epsilon_2 - 1}}, \quad (13b)$$

It is then possible to discuss both polarizations by writing

$$E_i' = F(z) F(z_i) E_{\infty i} q, \quad (14)$$

where E_i' denotes either E_{z_i}' or E_{ϕ_i}' and $F(z)$ denotes either $F_v(z)$ or $F_h(z)$ for vertical or horizontal polarization, respectively. The quantity q then stands for

$$q = \begin{cases} 1, & \text{for vertical polarization,} \\ \cos \phi_i, & \text{for horizontal polarization.} \end{cases} \quad (15)$$

The total field E' (i.e., either E_z' or E_ϕ') is obtained by superposition of all partial fields E_i' , so that

$$E' = \sum_{i=1}^n E_i', \quad (16)$$

where n is the total number of elements in the array.

Because we are concerned only with the far field within the layer $0 < z < h$, we may assume that $\phi_i \approx \phi$ and

$$\rho_i \approx \rho - x_i \cos \phi. \quad (17)$$

As usual, we may take $\rho = \rho_i$ in the amplitude but we must retain the form of Eq. (17) in the phase terms of E_i' . Inserting these approximations into Eq. (14) and then substituting the result into Eq. (16), one obtains

$$E' = \frac{60 q F(z) e^{-j k_0 [\rho + \sqrt{\epsilon_1 - 1} (h - z)]}}{(\epsilon_1 - 1) \rho^2} \sum_{i=1}^n \bar{I}_i l_i F(z_i) e^{j k [x_i \cos \phi - \sqrt{\epsilon_1 - 1} (h - z_i)]} \quad (18)$$

If the ground and vegetation layer were absent, the free-space field E at (ρ, ϕ, z) within the layer region $0 < z < h$ would have been given by

$$E = \frac{60 \pi q e^{-jk_c \rho}}{\lambda_c \rho} \sum_{i=1}^n I_i l_i e^{jk_0 x_i \cos \phi} \quad (19)$$

where λ_0 is the wavelength in free space (or air). To find the terrain loss L_t , as defined in Eq. (7), it is necessary to calculate

$$L_t = 10 \log \left| \frac{R_0}{R'_0} \frac{E}{E'} \right|^2 \quad (20)$$

where R_0 and R'_0 denote the antenna impedance in the absence or presence of the ground and vegetation media, respectively. However, the value of R'_0 differs substantially from that of R_0 only if the antenna is less than $\lambda_0/2$ above ground and/or if a considerable amount of vegetation is located within a distance of $\lambda_0/2$ around the antenna. (2) Because $\lambda_0/2$ is about 2.5 feet, it is reasonable to assume that these immediate proximity effects are small, so that one may take that $R_0 \approx R'_0$, in which case Eq. (20) simplifies to

$$L_t = 20 \log \left| \frac{E}{E'} \right|. \quad (21)$$

It is now possible to obtain L_t for any given situation because all of the quantities for E and E' are known in Eqs. (18) and (19), respectively. However, one may further simplify the expression for L_t by noting that the orientation of the array axis is expected to be horizontal if the antenna is placed within the vegetation layer. This is due to the fact that, in this case, both the target and the antenna are located at heights z and z_0 that are small compared to the total range ρ of the path connecting the two terminals. Hence, a horizontal orientation of the array axis should enhance the directivity in the desired direction and is therefore the preferred orientation. For such a case, all z_i in Eq. (18) are equal to the height z_0 of the antenna axis above ground so that the z dependent terms may be taken out from the summation factor. The remaining summation is then identical to that of Eq. (19). ^{If then Eq. (19)} is divided into Eq. (18), one obtains

$$L_t = 20 \log \left| \frac{\pi (\epsilon_1 - 1) \rho}{\lambda_0} \cdot \frac{e^{jk_0 \sqrt{\epsilon_1 - 1} (2h - z - z_0)}}{F(z) F(z_0)} \right|, \quad (22)$$

(for $0 < z < h$).

This result is a relatively simple expression for the terrain loss L_t and it is qualitatively and quantitatively discussed in Section V.

B. Antenna Above Tree Tops

If the target is within the vegetation and the transmitting antenna is in the air region well above the tree tops, the propagation mechanism linking the two terminals is not a lateral wave but rather a refracted line-of-sight wave. (4) The line-of-sight mechanism, as shown by the segmented line T A R in Fig. 5, holds for all heights above the tree tops, with the exception of a relatively thin layer just above the tree tops. This small region possesses a thickness of about a wavelength or less and serves as a transition region between the lateral-wave regime inside the vegetation layer and the refracted line-of-sight regime in the air region.

Because the thickness of the transition region is of the order of one wavelength, the discussion will be restricted to the air region above the transition region. To evaluate the terrain loss L_t , it is again assumed that the axis of the array shown in Fig. 3 is located in the xz plane of Fig. 5. In the present case, however, a spherical coordinate system (r, θ, ϕ) is employed, with its origin at the point (x, y, h) , i. e., this origin is on the forest-air boundary at a point located directly above the target point R at (x, y, z) . In this case, the field E_i' produced at the target by a single dipole element located at (r_i, θ_i, ϕ_i) is given (5) by:

$$E_i' = j I_i l_i \frac{120\pi}{\lambda_0 r_i} \cdot \frac{pq \cos \theta_i}{m \cos \theta_i + \sqrt{\epsilon_1 - \sin^2 \theta_i}} S(\theta_i) e^{-jk_0 [r_i + \sqrt{\epsilon_1 - \sin^2 \theta_i} (h - z)]} \quad (23)$$

where q was defined in Eq. (15) and

$$S(\theta) = \frac{1 + \Gamma(\theta) e^{-2jk_0 \sqrt{\epsilon_1 - \sin^2 \theta} z}}{1 - \left(1 - \frac{2 \cos \theta}{m \cos \theta + \sqrt{\epsilon_1 - \sin^2 \theta}}\right) \Gamma(\theta) e^{-2jk_0 \sqrt{\epsilon_1 - \sin^2 \theta} h}} \quad (24)$$

$$\Gamma(\theta) = \begin{cases} \frac{\epsilon_2 \sqrt{\epsilon_1 - \sin^2 \theta} - \epsilon_1 \sqrt{\epsilon_2 - \sin^2 \theta}}{\epsilon_2 \sqrt{\epsilon_1 - \sin^2 \theta} + \epsilon_1 \sqrt{\epsilon_2 - \sin^2 \theta}} & \text{(for vert. pol.) ,} \\ \frac{\sqrt{\epsilon_1 - \sin^2 \theta} - \sqrt{\epsilon_2 - \sin^2 \theta}}{\sqrt{\epsilon_1 - \sin^2 \theta} + \sqrt{\epsilon_2 - \sin^2 \theta}} & \text{(for hor. pol.) ,} \end{cases} \quad (25)$$

$$p = \begin{cases} \sin^2 \theta_i & , \text{ for vertical polarization ,} \\ 1 & , \text{ for horizontal polarization ,} \end{cases} \quad (26)$$

$$m = \begin{cases} \epsilon_1 & , \text{ for vertical polarization ,} \\ 1 & , \text{ for horizontal polarization .} \end{cases} \quad (27)$$

Taking $r_i \approx r$ and $\theta_i \approx \theta$ in the amplitude terms but leaving r_i unchanged in the phase, one obtains for the total field at the target

$$E' = j \frac{120\pi}{\lambda_0 r} \frac{pq \cos \theta}{m \cos \theta + \sqrt{\epsilon_1 - \sin^2 \theta}} S(\theta) e^{-jk_0 \sqrt{\epsilon_1 - \sin^2 \theta} (h-z)} \times \sum_{i=1}^n I_i l_i e^{-jk_0 r_i} \quad (28)$$

On the other hand, if unbounded free space replaces both the ground and the forest layer, the field is given by

$$E = \frac{60\pi}{\lambda_0} pq \sum_{i=1}^n \frac{I_i l_i e^{-jk_0 R_i}}{R_i} \quad (29)$$

where R_i is the distance between the dipole element at $(x_i, 0, z_i)$ and the target at (x, y, z) . Equation (29) has assumed the far-field approximation $\theta_i = \theta$ and $\phi_i = \phi$. One may now introduce the approximation $R_i = r$ in the amplitude and, for the phase terms, replace R_i with

$$R_i = r_i + (h-z) \cos \theta \quad , \quad (30)$$

thus obtaining

$$E \approx \frac{60\pi}{\lambda_0} p_{eq} e^{-jk_c(h-z)\cos\theta} \sum_{i=1}^n \frac{I_i l_i e^{-jk_e r_i}}{r} \quad (31)$$

By dividing Eq. (31) through Eq. (28), we obtain

$$L_t = 20 \log \left| \frac{m \cos \theta + \sqrt{\epsilon_1 - \sin^2 \theta}}{2 \cos \theta} \cdot \frac{e^{jk_c \sqrt{\epsilon_1 - \sin^2 \theta} (h-z)}}{S(\theta)} \right| \quad , \quad (32)$$

(for $z > h$).

Unlike the result for L_t in Eq. (20), which holds when the antenna is within the vegetation layer, the result in Eq. (32) is not restricted to an array whose axis is horizontal. By combining the results in Eqs. (22) and (32), one may evaluate the terrain loss L_t for any height of the antenna, and thus obtain the variation of L_t as the antenna is raised from a position near the ground to large heights above the tree tops. The actual variation of L_t is evidently continuous; however, at $z = h$, the calculated value of L_t will be discontinuous, but this occurs only because Eq. (32) for an antenna in the air region does not strictly hold at and close to $z = h$. It is recalled that a transition region holds between $z = h$ and $z = h + \lambda_0$; within this layer of thickness equal roughly to λ_0 , L_t may be well approximated by interpolating between the value of L_t at $z = h$, as obtained from Eq. (22), and the value of L_t at $z = h + \lambda_0$, as obtained from Eq. (32).

Quantitative results for L_t according to the formulas derived here are carried out for horizontal polarization in the following sections.

V. TERRAIN LOSS CALCULATIONS

As discussed above, the terrain loss L_t may be found for the class of situations considered here by employing Eqs. (22) or (32). These relations may be used for any antenna height (provided $z > \lambda_0/2$), any frequency f within $2 < f < 200$ MHz, and for either vertical or horizontal polarization. However, for the purposes of this report, curves for L_t will be derived for the conditions stipulated in Section II, namely; for horizontal polarization, $f = 140$ MHz and a height of the target $z = 1$ m, above ground.

It is interesting to note that, as discussed in Section III, neither the antenna gain G nor the scattering cross section σ of the target appear explicitly in L_t . Hence, the results found here apply to any value of G or σ , the only restrictions on these quantities being those already described in Sections III and IV.

A. Classification of Forest Parameters

The calculations of L_t involve the important complex parameter ϵ_1 , this being the relative permittivity of the vegetation medium. This parameter may be written as

$$\epsilon_1 = \epsilon' (1 - j \tan \delta), \quad (33)$$

where ϵ' is the real part of the relative permittivity, whereas $\tan \delta$ refers to the loss factor of the dielectric material. An examination of available data⁽⁶⁾ suggests that it is convenient to classify vegetation into three representative varieties as given below:

	ϵ'	$\tan \delta$	$\epsilon_1 - 1$
Sparse vegetation	1.01	.01	0.01 (1-j)
Medium "	1.03	.03	0.03 (1-j)
Thick "	1.10	.1	0.1 (1-j)

Note that the above classification is different from that adopted with respect to forests in reference 2. The present classification applies to 140 MHz and refers to the vegetation medium only; it does not include the tree height and the ground parameters. Furthermore, the values in the above table are closer to values that were actually measured near the frequency under consideration.

Although, in general, one also needs to know the relative complex permittivity ϵ_2 of the ground, this quantity plays only a secondary role in the case of horizontal polarization so that exact values of ϵ_2 are unimportant. On the other hand, the average height h of the trees has a very strong effect on L_t and calculations are therefore carried out for $h = 5, 10, 15$ and 20 meters to cover a wide range of forests.

B. Antenna Within Vegetation Layer

In general, the ground permittivity is much larger than the vegetation permittivity, i. e., $|\epsilon_2| \gg |\epsilon_1|$, so that Eq. (13b) yields the approximation

$$\Gamma_h \approx -1 \quad (34)$$

Inserting this into Eq. (12), one gets

$$\Gamma_h(z) = j \frac{\sin k_0 \sqrt{\epsilon_1 - 1} z}{\cos k_0 \sqrt{\epsilon_1 - 1} h} e^{j k_0 \sqrt{\epsilon_1 - 1} (h-z)} \quad (35)$$

Hence, Eq. (22) yields

$$L_t = 20 \log \left| \frac{\pi (\epsilon_1 - 1) a}{\lambda_0} \frac{\cos^2 k_0 \sqrt{\epsilon_1 - 1} h}{\sin k_0 \sqrt{\epsilon_1 - 1} z \sin k_0 \sqrt{\epsilon_1 - 1} z_0} \right| \quad (36)$$

For calculation purposes, it is convenient to define

$$L(\rho) = 20 \log \frac{\pi |\epsilon_1 - 1| \rho}{\lambda_0}, \quad (37)$$

$$L(h) = 20 \log \left| \cos k_0 \sqrt{\epsilon_1 - 1} h \right|, \quad (38)$$

$$L(z) = -20 \log \left| \sin k_0 \sqrt{\epsilon_1 - 1} z \right|, \quad (39)$$

so that

$$L_t = L(\rho) + 2L(h) + L(z) + L(z_0). \quad (40)$$

The values of $L(\rho)$, $L(h)$ and $L(z)$ are given in Figs. 6, 7 and 8, respectively. Hence, the terrain loss L_t may be found from Eq. (40) and from Figs. 6, 7 and 8 for any suitable combination of the parameters ρ , h and z . Specific examples are discussed below in Section D of the present Chapter.

C. Antenna Above Vegetation Layer

As in the case of Γ_h of Eq. (34), when the condition $|\epsilon_2| \gg |\epsilon_1|$ is introduced in Eq. (25), one obtains the approximation

$$\Gamma(\theta) \approx -1, \quad (41)$$

in the case of horizontal polarization. Furthermore, one has then $m = p = 1$. To find $S(\theta)$ of Eq. (24), it is first noted that the second term (containing $\cos \theta$) within the round brackets in the denominator is small compared to unity for most practical values ($\cos \theta < 0.1$). If this term is neglected, one obtains

$$S(\theta) \approx -j \frac{\sin k_0 \sqrt{\epsilon_1 - 1} z}{\cos k_0 \sqrt{\epsilon_1 - 1} h} e^{jk_0 \sqrt{\epsilon_1 - 1} (h-z)}. \quad (42)$$

Inserting this result into Eq. (32), one gets

$$L_t = 20 \log \left| \frac{\cos \theta + \sqrt{\epsilon_1 - \sin^2 \theta}}{2 \cos \theta} \cdot \frac{\cos k_0 \sqrt{\epsilon_1 - 1} h}{\sin k_0 \sqrt{\epsilon_1 - 1} z} \right| \quad (43)$$

By defining

$$L(\theta) = 20 \log \left| \frac{\cos \theta + \sqrt{\epsilon_1 - \sin^2 \theta}}{2 \cos \theta} \right| = 20 \log \left| \frac{1}{2} (1 + \sqrt{(\epsilon_1 - 1) \sec^2 \theta + 1}) \right|, \quad (44)$$

the terrain loss becomes

$$L_t = L(\theta) + L(h) + L(z), \quad (45)$$

where $L(h)$ and $L(z)$ were already defined in Eqs. (38) and (39), respectively.

The values of $L(\theta)$ are given in Fig. 9 in terms of $\sec \theta$. As in the case of the antenna within the forest layer discussed previously, L_t may be found by means of Eq. (45) and the curves given in Figs. 7, 8 and 9 for any combination of the parameters ρ , h and z . Specific examples are discussed below in Sec. D of the present Chapter.

D. Antenna Height Gain

The advantage of raising the height of the antenna has been well documented.⁽¹⁻⁵⁾ In the case under consideration, increasing the height z_o of the antenna above ground has the effect of decreasing the terrain loss. This decrease in L_t with z_o may readily be calculated by means of Figs. 7-9.

To illustrate the effect of changing the antenna height z_o , the terrain loss L_t was calculated and displayed in Figs. 10-13 for a distance $\rho = 500$ m. between the antenna and the target, for various forest heights h and for the three varieties of foliage enumerated in Section A of the present Chapter. As expected, Figs. 10-13 show that L_t is largest for dense forest and smallest for sparse foliage, with the average foliage being associated with intermediate values of L_t . Also, L_t increases with the forest height h ; this behavior is also expected because the height z of the target is fixed at $z = 1$ m. above ground. Hence, both the lateral-wave segment BR in Fig. 4 and the refracted-wave segment A'R in Fig. 5 increase as h increases, thus adding losses in the way of the incoming signal.

Another result illustrated in Figs. 10-13 is that L_t may become prohibitively large for thick foliage and $h > 10$ m. Thus, in Figs. 11-13 it is noted that L_t is about 80 dB or larger unless the antenna height is raised well above the thick foliage. Recalling that L_t is only the one-way loss in sensitivity due to the terrain, it would be practically impossible to detect a target at 500 m. if the antenna is located below the height h in thick foliage situations. However, targets at $\rho < 500$ m. may still be detected, as discussed in the following section.

E. Variation of L_t with the Range ρ .

The preceding considerations for Figs. 10-13 were relevant to a fixed value $\rho = 500$ m. For ranges different from 500 m., L_t may be smaller or larger depending whether ρ is shorter or longer than 500 m., respectively.

For antennas located within the vegetation layer, the value of L_t may easily be found from Figs. 10-13 with the help of Fig. 6. Because only $L(\rho)$ changes with ρ in that case, one may readily obtain L_t for any ρ if L_t is known for $\rho = 500$ m. It is also pertinent to note that $L(\rho)$ has a slope of 20 dB per decade, thus making all these calculations very simple.

For antennas located above the tree tops, the range variation is given by $L(\theta)$ of Fig. 9, which was calculated from Eq. (44). However, for values of $\sec \theta$ that are sufficiently large, Eq. (44) may be approximated by

$$L(\theta) \simeq 20 \log \left| \frac{\sqrt{\epsilon_1 - 1}}{2} \sec \theta \right| \simeq 20 \log \frac{|\sqrt{\epsilon_1 - 1}|}{2} \frac{\rho}{z_0 - h} \quad (46)$$

Because of the presence of ρ in the last result, $L(\theta)$ also varies with a slope of 20 dB per decade in the same manner as $L(\rho)$, provided $\sec \theta$ is large enough.

To illustrate the above considerations, L_t is given in Fig. 14 as a function of ρ for a forest height $h = 10$ m. with medium foliage, and for various antenna heights z_0 . It is noted therein that the linear behavior of L_t on a logarithmic scale for ρ holds for most ranges of practical interest. It therefore follows that, with the help of Fig. 9, the values of L_t may be found from Figs. 10-13 for almost any situation. The exceptions occur at those values of ρ and $z_0 > h$ for which the ratio $\rho / (z_0 - h)$ is smaller than about 5.

VI. VEGETATION LOSS CALCULATIONS

Whereas the terrain loss L_t yields a large amount of information on the effects of both ground and foliage, the effect of vegetation alone may serve as a more convenient measure in certain situations. As already defined in Eq. (9), the vegetation loss L_{veg} represents the system sensitivity loss due to both vegetation and ground, as compared to the sensitivity loss L_{gr} in the presence of a bare ground only. Because of this definition, L_{veg} may be measured directly by comparing the results of two measurements, one of which involves the detection of a target on a bare ground whereas the other involves the detection of the same target and at the same range, antenna height, etc., but under conditions such that a forest layer covers the ground.

To calculate L_{veg} , it is possible to use the previously derived results given in Figs. 10-14 provided L_{gr} is known. If L_{gr} is available, L_{veg} is found from Eq. (9), wherein L_t is available already in Figs. 10-14. The sensitivity loss L_{gr} is generally dependent on the particular ground constants. However, for horizontal polarization, most grounds may be assumed to be perfectly reflecting,⁽⁷⁾ as already discussed in Chapter IV. In that case, the sensitivity loss L_{gr} is due only to the ground-lobing effect on the antenna pattern, which corresponds to a loss⁽⁷⁾

$$\frac{E}{E''} = -20 \log \left(2 \sin \frac{k_o z_o}{\rho} \right) \quad , \quad (47)$$

where E and E'' refer to fields without and with the reflecting ground, respectively. Quantitative results for Eq. (47) are given in Fig. 15, which is restricted to those values of ρ and z_o for which the sine term in Eq. (47) may be approximated by its argument, i.e., for $k_o z_o / \rho \ll 1$.

By using the relation $L_{veg} = L_t - L_{gr}$ already given in Eq. (9), all of the curves in Figs. 10-13 were replotted for L_{veg} in Figs. 16-19, respectively. Although Figs. 16-19 were calculated for a nominal distance $\rho = 500$ m., the results hold for a much larger range. This is due to the fact that, for

$k_o z z_o \ll 1$, both L_{gr} and L_t contain a term $\log \rho$, so that their difference is then independent on the range ρ . In the present case, one has

$$\frac{k_o z z_o}{\rho} = 2\pi \frac{z z_o}{\lambda_o \rho} = \frac{2\pi}{2.15} \cdot \frac{z_o}{\rho} = 2.92 \frac{z_o}{\rho}, \quad (48)$$

so that, to a good approximation, the results given in Figs. 16-19 hold for all $\rho / z_o > 3$.

An interesting feature of Figs. 16-19 is that, upon comparing these with Figs. 10-13, one notices that the height gain effect is less pronounced for L_{veg} in comparison to L_t . This is quite expected because L_{veg} views the height gain with respect to the situation over bare ground, which also exhibits a pronounced height gain. The difference between the two situations is therefore smaller than that which occurs for L_t with respect to free space. Nevertheless, a considerable height gain is also evident for $z > h$ in the case of L_{veg} , especially in the case of thicker vegetations.

The curves given in Figs. 16-19 lend themselves readily to experimental verification. If such a verification is carried out and the agreement is good, these curves could be employed to obtain system performance predictions for a large variety of terrain conditions. Alternatively, the same curves could be employed to determine the parameters of vegetation, thus serving to identify the electrical characteristics of foliage - a measurement that cannot otherwise be easily carried out.

VII. CONCLUSIONS

The effect of a forest environment on a Doppler remote sensing system was examined. It was shown that, if comparison is made with the same system under free space conditions, the presence of a forest environment may be expressed in terms of a single quantity in the form of a sensitivity loss L_t . This loss, termed terrain loss, is a function of the distance ρ separating the antenna from the target, the heights z_o and z of the antenna and the target, respectively, the average tree height h , as well as the electrical characteristics of the foliage and ground. To a first approximation, the loss L_t is not dependent on either the antenna gain G or the radar cross section σ of the target. This independence of L_t on G and σ makes the use of L_t particularly attractive.

For horizontal polarization, the terrain loss L_t was calculated for a large range of the parameters ρ , z_o and h . It was shown that the loss L_t increases with ρ and h , but decreases with z_o , in agreement with the known physical characteristics of the wave propagation mechanism. This mechanism is given by a lateral wave if both the antenna and the target are inside the forest, or by a refracted line-of-sight wave if the antenna is outside the vegetation layer.

The forest environment was characterized in terms of two principal parameters: the average tree height h , on the one hand, and the density of the foliage, on the other hand. In this manner, the terrain loss L_t was determined for a large number of typical forests, which include tree heights between 5 to 20 meters and foliage densities that may be sparse, medium or thick. In this manner, predictions of operation conditions under a large variety of forests may be obtained. Whereas these predictions are still subject to experimental verification, previous successful modelling work based on the assumptions utilized here suggests that the present quantitative results represent very plausible estimates.

For the purpose of experimental verification, a loss parameter L_{veg} was introduced, which represents the effect of vegetation when the performance of

the system is compared to that in the presence of bare ground. This vegetation loss L_{veg} is readily measurable for any given system and thus facilitates greatly the final determination of the sensitivity loss L_t . For horizontal polarization, L_{veg} is not dependent on the distance ρ for practical values of z and z_o , thus further simplifying the measurement procedure.

Although the quantitative results presented here were restricted to a frequency $f = 140$ MHz. and a target height $z = 1$ m., the derivations obtained are general and data could be obtained for any other heights z of the target and for any frequency within the range 2 - 200 MHz. In that context, it is suggested that a study be undertaken to evaluate the advantages of operating at frequencies other than that of 140 MHz, giving due considerations to the antenna gain and to other parameters whose practical value is strongly dependent on the particular frequency chosen.

References

1. T. Tamir, "On Radio Wave Propagation in Forest Environments", IEEE Trans. on Antennas and Propagation, vol. AP-15, pp. 806-817; November 1967.
2. D. Dence and T. Tamir, "Radio Loss of Lateral Waves in Forest Environments", Radio Sci., vol. 4, pp. 307-318; April 1969.
3. L.G. Sturgill and Staff, "Tropical Propagation Research", Atlantic Research, Jansky and Bailey Engng. Div., Final Report, vol. II, 1969.
4. T. Tamir, "On the Electromagnetic Field Radiated Above the Tree Tops by an Antenna Located in a Forest", U.S. Army Electronics Command, Ft. Monmouth, N.J., Res. & Devp. Tech. Rept. ECOM-3443; June 1971.
5. T. Tamir, personal notes.
6. H.W. Parker and W. Makarabhiromya, "Electric Constants Measured in Vegetation and in Earth at Five Sites in Thailand", Stanford Research Inst., Special Tech. Rept. 43; December 1967.
7. L.N. Ridenour, "Radar System Engineering", (McGraw-Hill, N.Y. 1947), sec. 2.12, pp. 47-53.

List of Figures

- Fig. 1. Schematic outline of a forest environment.
- Fig. 2. Slab model of a forest environment.
- Fig. 3. Antenna dipole array model.
- Fig. 4. Geometry of the forest model for an antenna within the vegetation layer. The path traversed by the lateral wave from the i^{th} dipole to the target is given by the trajectory TABR.
- Fig. 5. Geometry of the forest model for an antenna above the tree tops. The path traversed by the refracted line-of-sight wave from the i^{th} dipole to the target is given by the trajectory TA'R.
- Fig. 6. Range loss $L(\rho)$ versus ρ for various types of vegetation.
- Fig. 7. Tree height loss $L(h)$ versus h for various types of vegetation.
- Fig. 8. Elevation loss $L(z)$ versus z for various types of vegetation.
- Fig. 9. Angular loss $L(\theta)$ versus θ for various types of vegetation.
- Fig. 10. Terrain loss L_t versus antenna height z_o for various types of vegetation. Results shown are for a range $\rho = 500$ m., average tree height $h = 5$ m. and target height $z = 1$ m.
- Fig. 11. Terrain loss L_t versus antenna height z_o for various types of vegetation. Results shown are for a range $\rho = 500$ m., average tree height $h = 10$ m. and target height $z = 1$ m.
- Fig. 12. Terrain loss L_t versus antenna height z_o for various types of vegetation. Results shown are for a range $\rho = 500$ m., average tree height $h = 15$ m. and target height $z = 1$ m.
- Fig. 13. Terrain loss L_t versus antenna height z_o for various types of vegetation. Results shown are for a range $\rho = 500$ m., average tree height $h = 20$ m. and target height $z = 1$ m.

List of Figures (Cont' d)

- Fig. 14. Terrain loss L_t versus range ρ for various antenna heights z_o . Results shown are for a forest with medium foliage and an average tree height $h = 10$ m.
- Fig. 15. Bare ground loss L_{gr} versus range ρ for various antenna heights z_o .
- Fig. 16. Vegetation loss L_{veg} versus antenna height z_o for various types of vegetation. Results shown are for an average tree height $h = 5$ m. and target height $z = 1$ m.; the range ρ may take on any value larger than $\rho_{min} \approx 3 z_o$.
- Fig. 17. Vegetation loss L_{veg} versus antenna height z_o for various types of vegetation. Results shown are for an average tree height $h = 10$ m. and target height $z = 1$ m.; the range ρ may take on any value larger than $\rho_{min} \approx 3 z_o$.
- Fig. 18. Vegetation loss L_{veg} versus antenna height z_o for various types of vegetation. Results shown are for an average tree height $h = 15$ m. and target height $z = 1$ m.; the range ρ may take on any value larger than $\rho_{min} \approx 3 z_o$.
- Fig. 19. Vegetation loss L_{veg} versus antenna height z_o for various types of vegetation. Results shown are for an average tree height $h = 20$ m. and target height $z = 1$ m.; the range ρ may take on any value larger than $\rho_{min} \approx 3 z_o$.

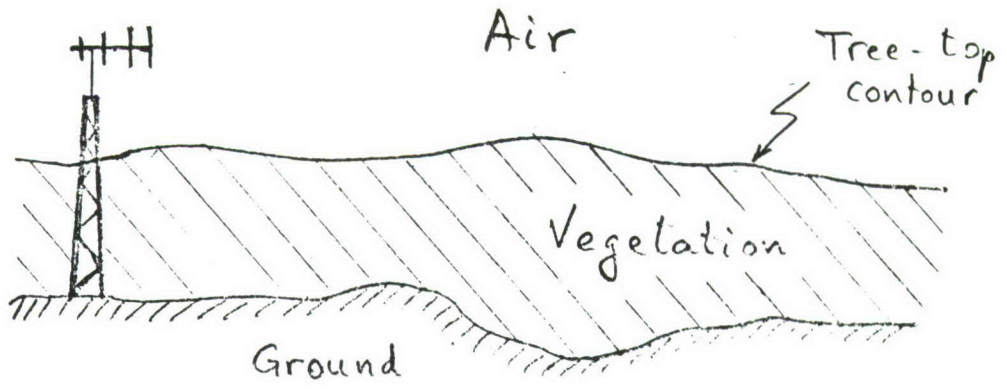


Fig. 1. Schematic outline of a forest environment.

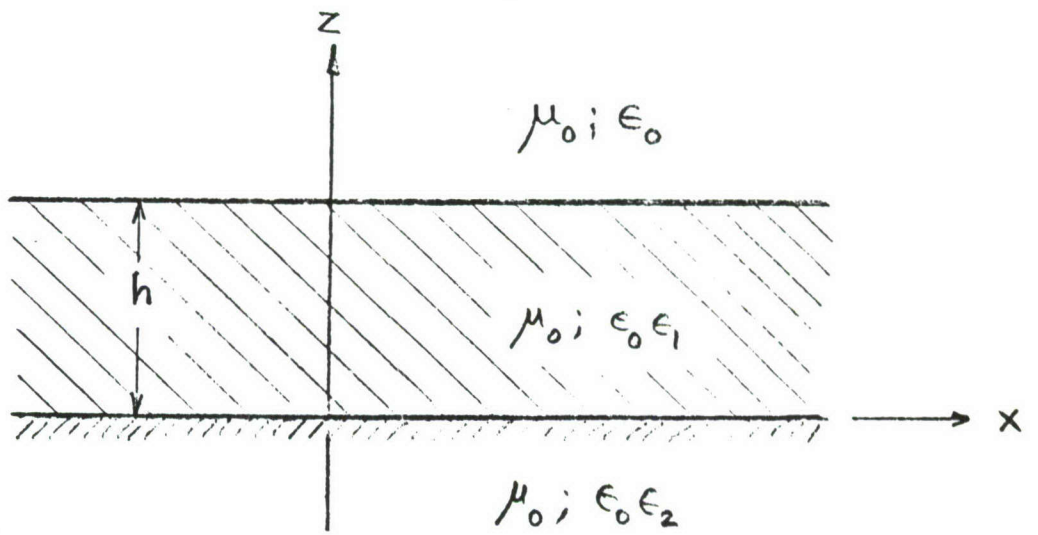


Fig. 2. Slab model of a forest environment.

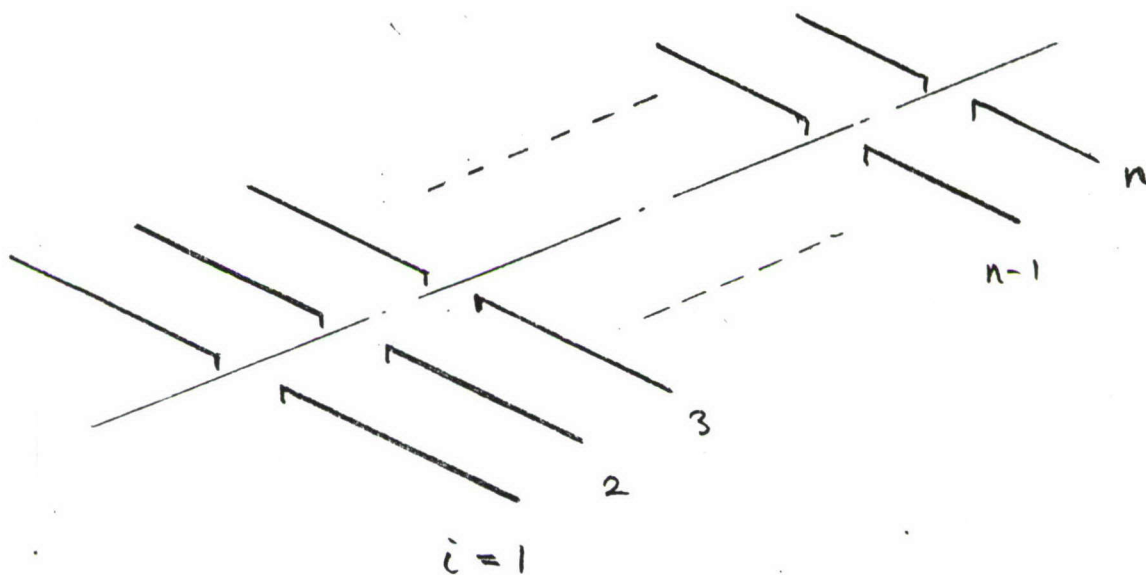


Fig. 3. Antenna dipole array model.

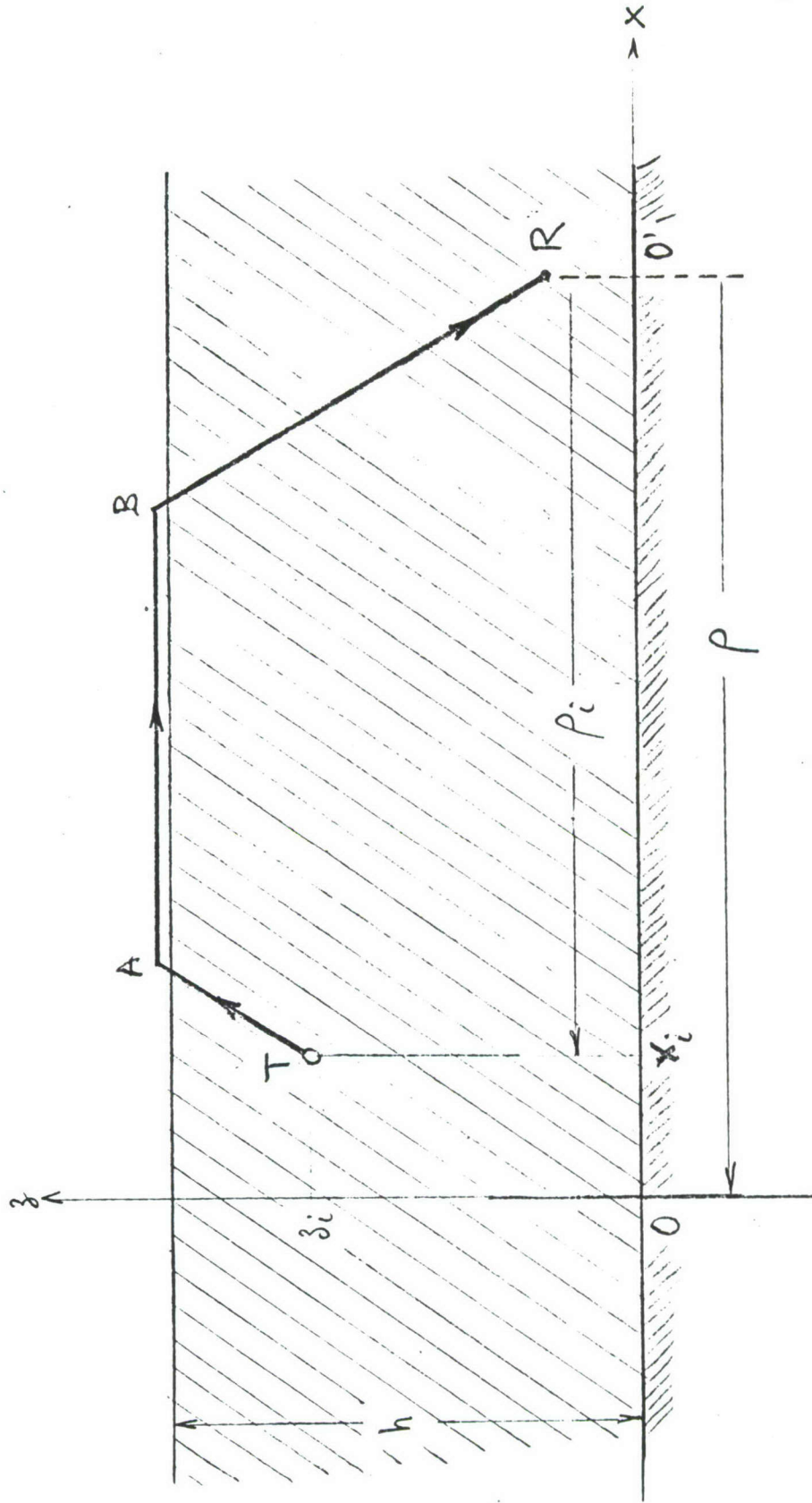


Fig. 4. Geometry of the forest model for an antenna within the vegetation layer. The path traversed by the lateral wave from the i^{th} dipole to the target is given by the trajectory TABR.

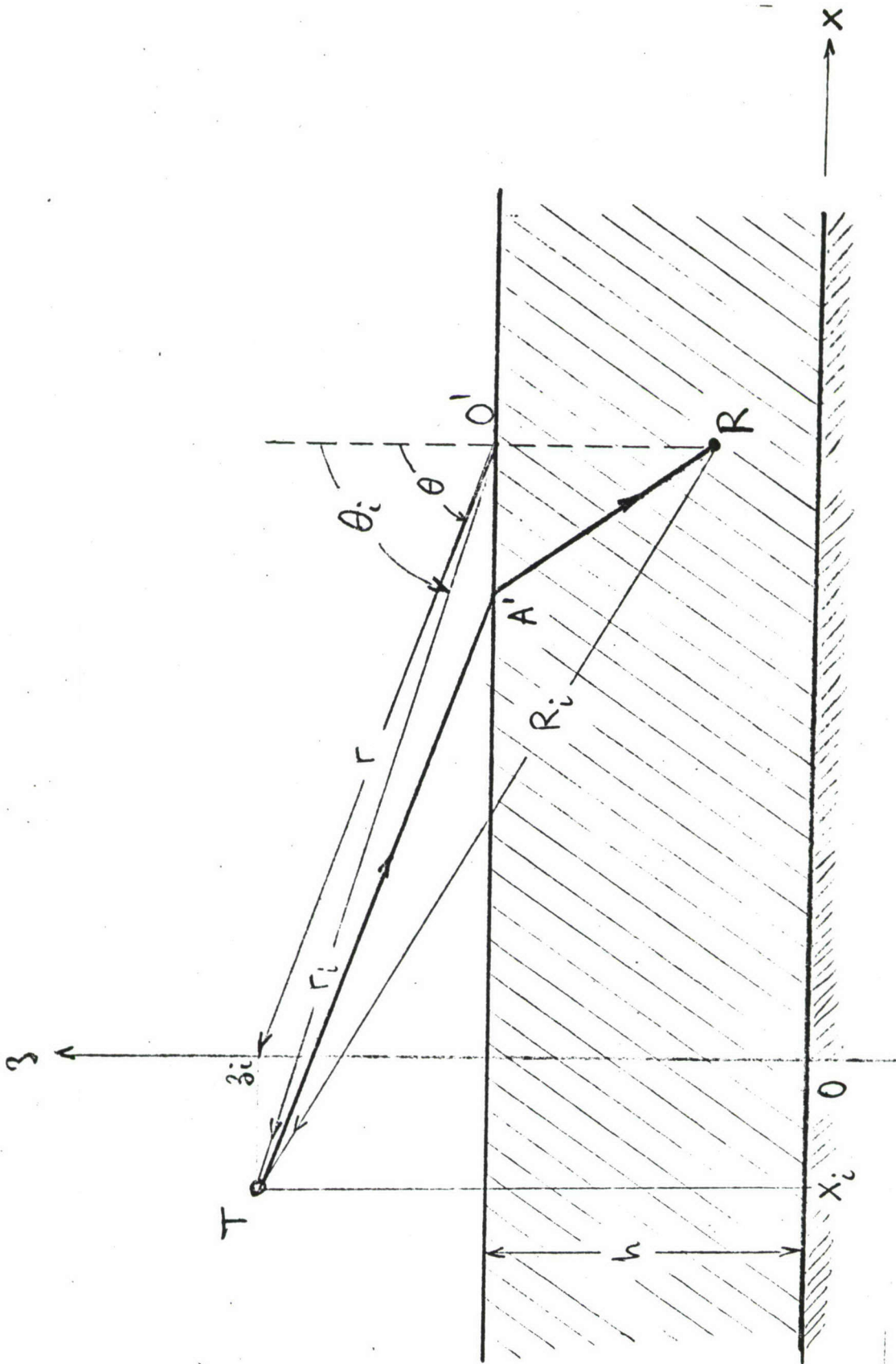


Fig. 5. Geometry of the forest model for an antenna above the tree tops. The path traversed by the refracted line-of-sight wave from the i^{th} dipole to the target is given by the trajectory $TA'R$.

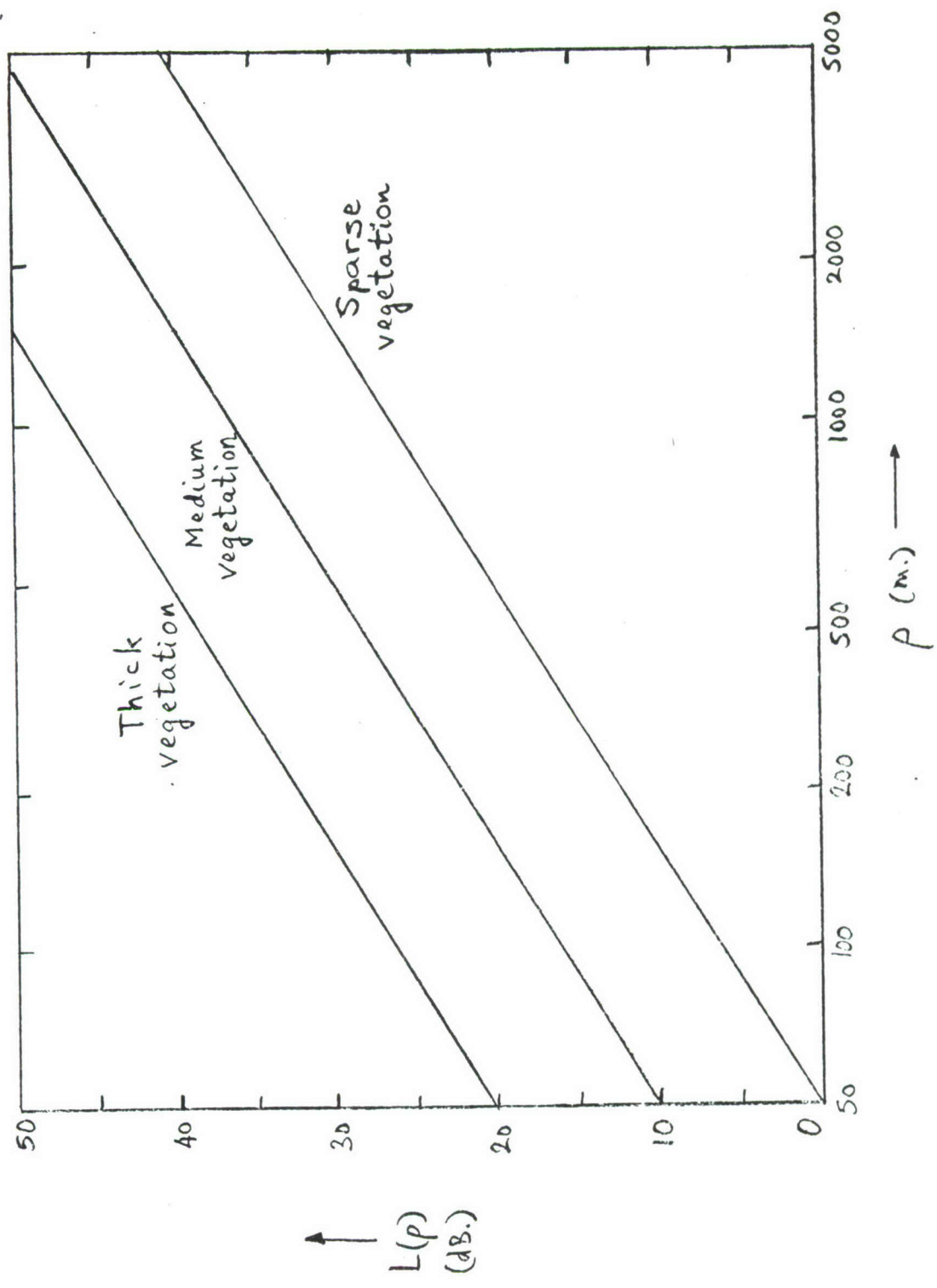


Fig. 6. Range loss $L(\rho)$ versus ρ for various types of vegetation.

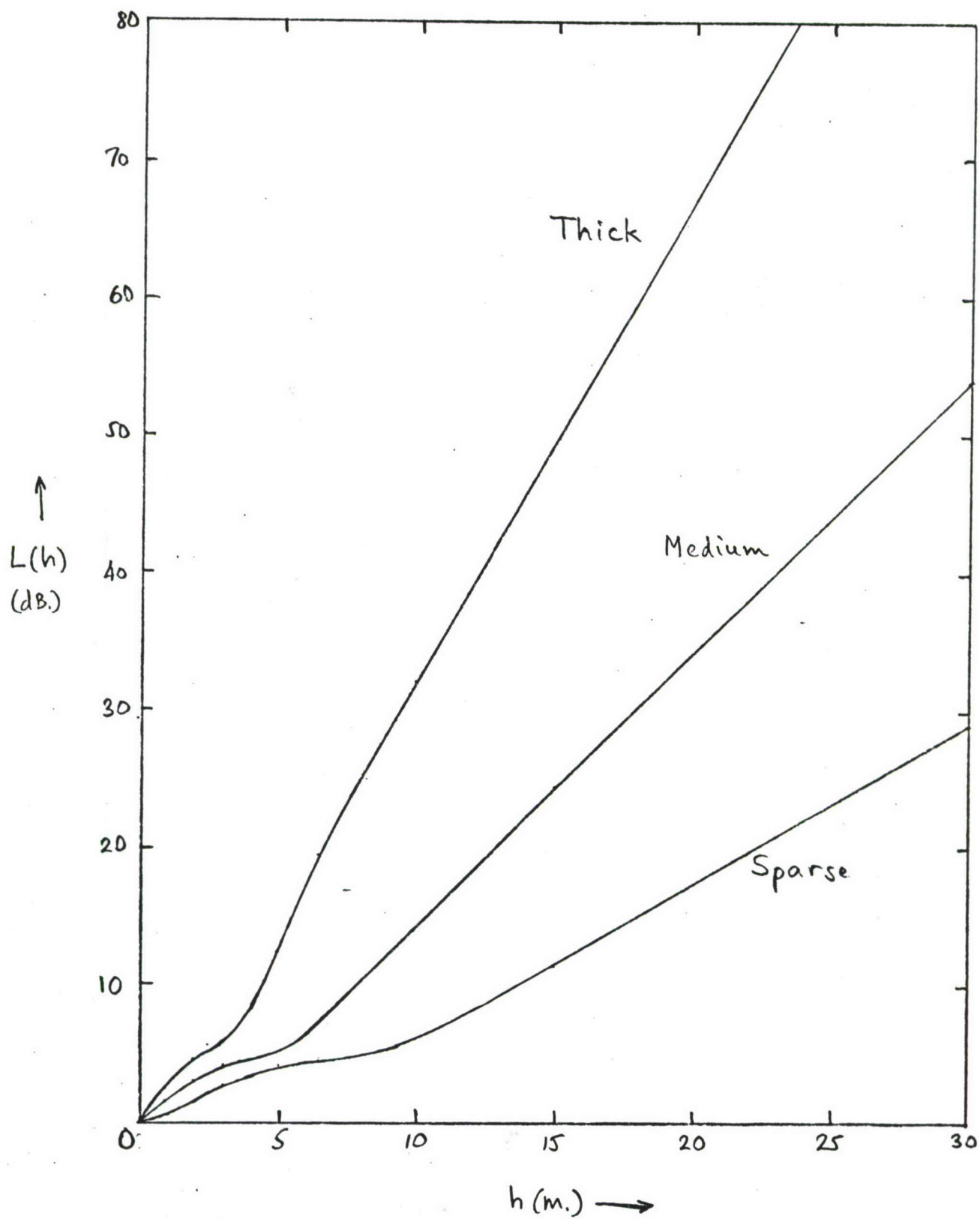


Fig. 7. Tree height loss $L(h)$ versus h for various types of vegetation.

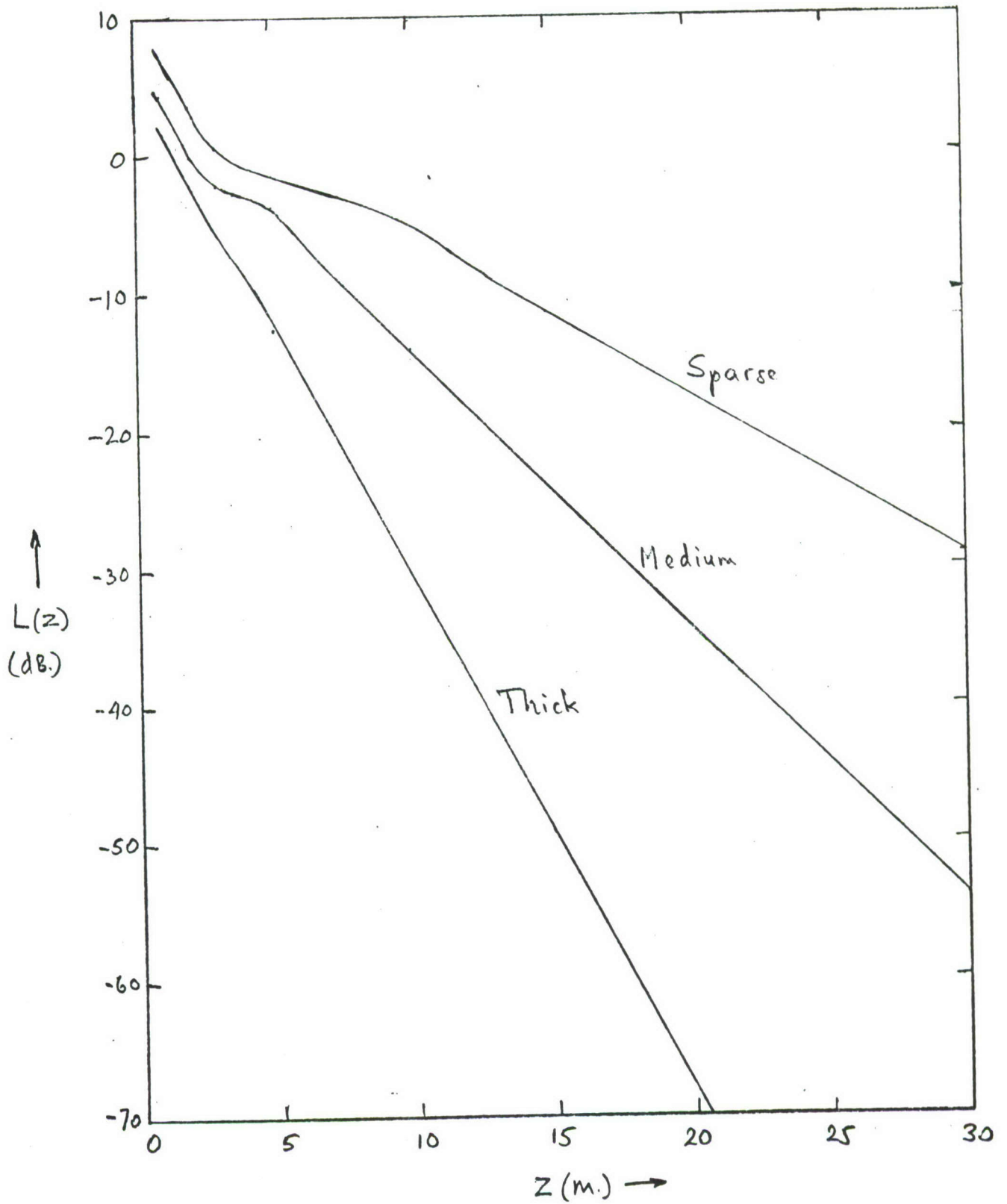


Fig. -8. Elevation loss $L(z)$ versus z for various types of vegetation.

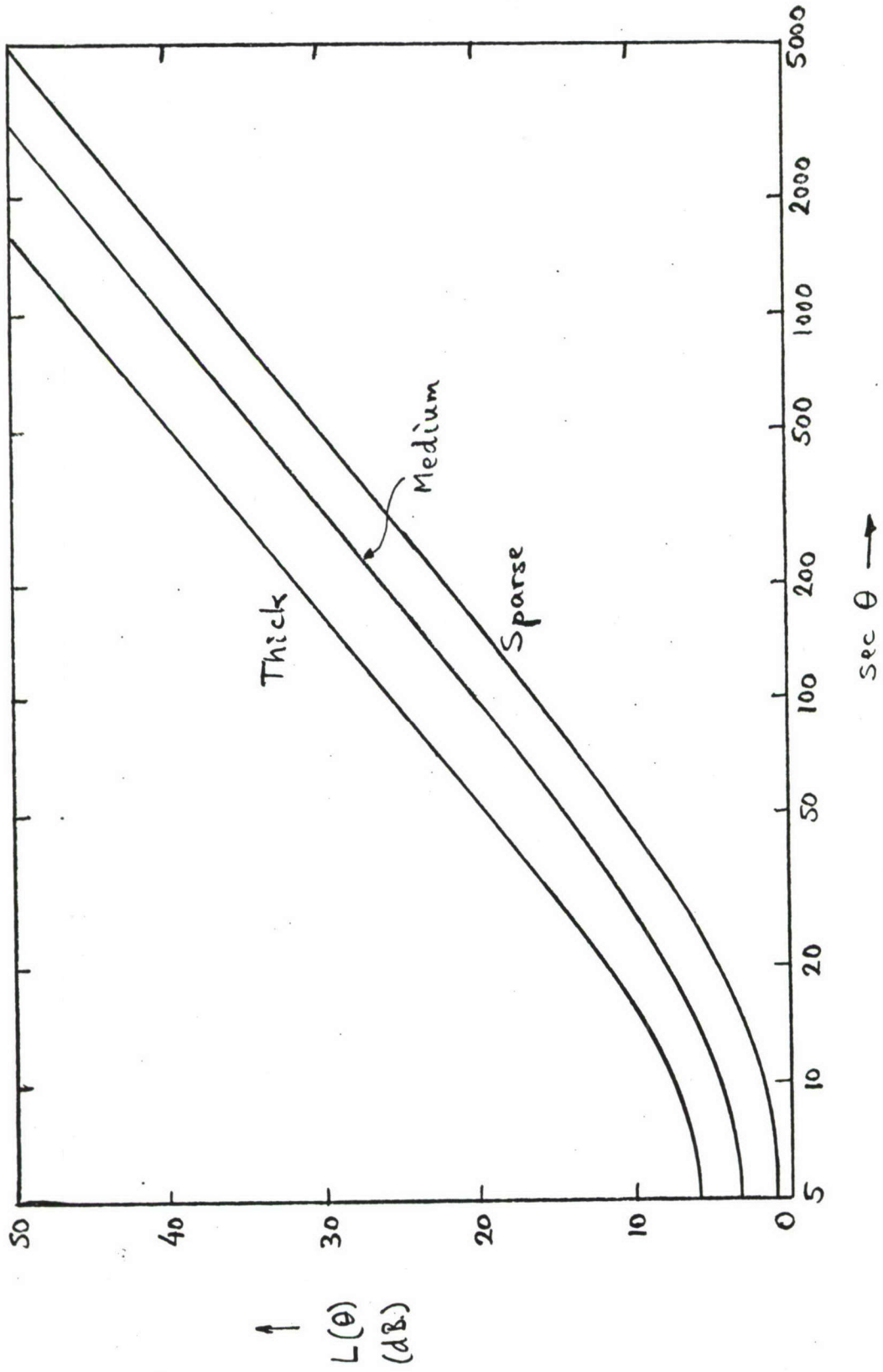


Fig. 9. Angular loss $L(\theta)$ versus θ for various types of vegetation.

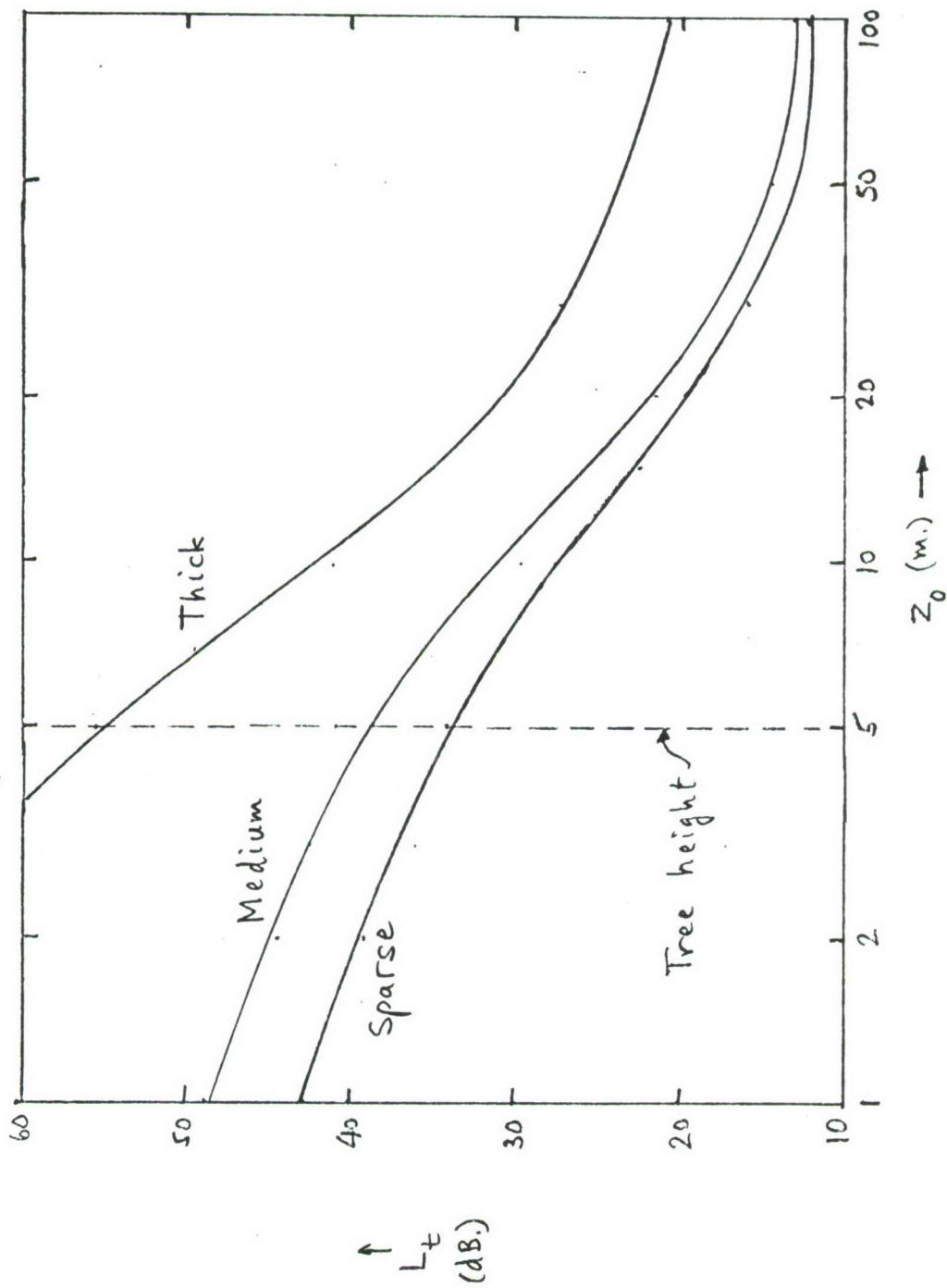


Fig. 10. Terrain loss L_t versus antenna height z_0 for various types of vegetation. Results shown are for a range $\rho = 500$ m., average tree height $h = 5$ m. and target height $z = 1$ m.

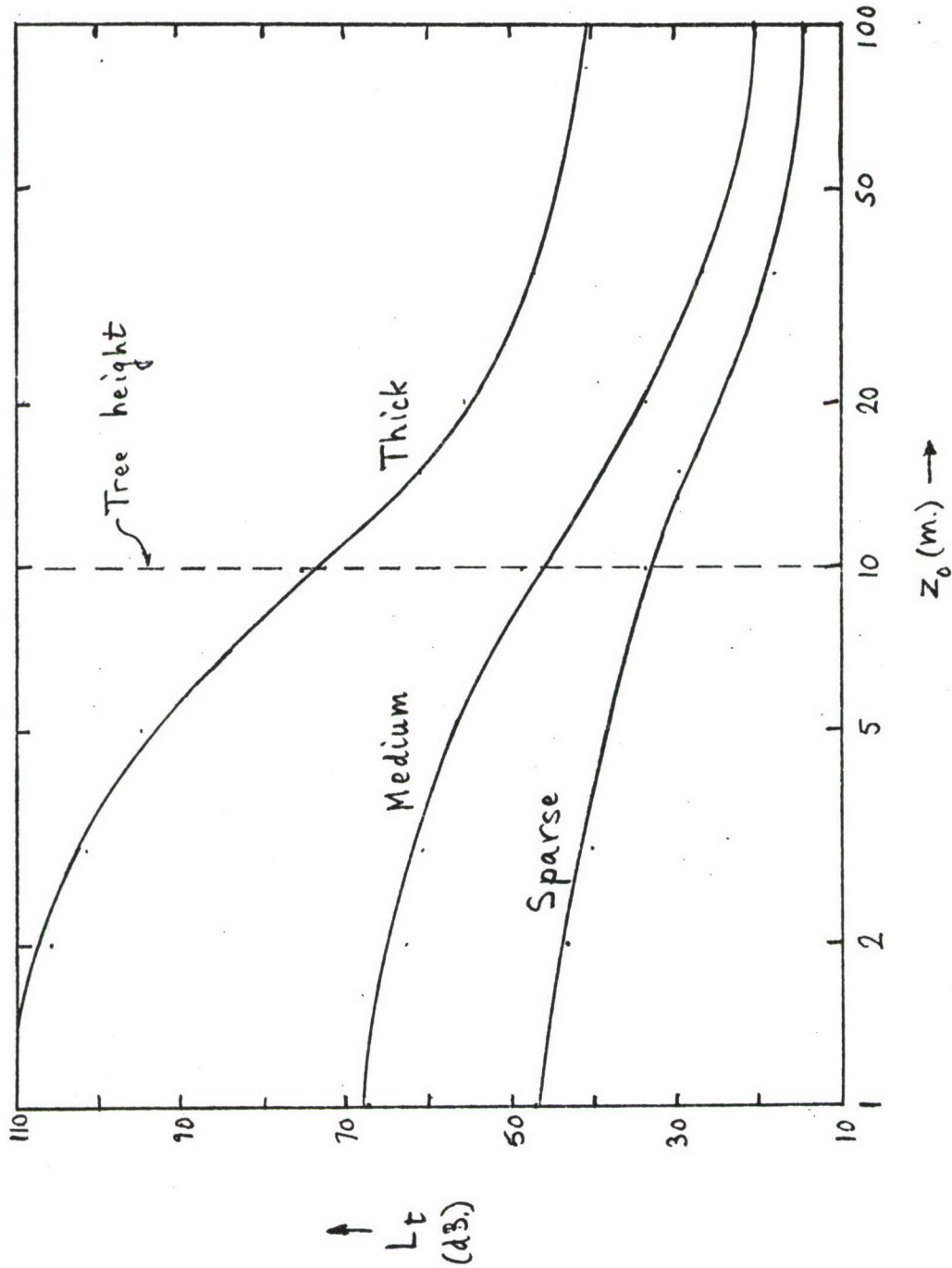


Fig. 11. Terrain loss L_t versus antenna height z_0 for various types of vegetation. Results shown are for a range $\rho = 500$ m., average tree height $h = 10$ m. and target height $z = 1$ m.

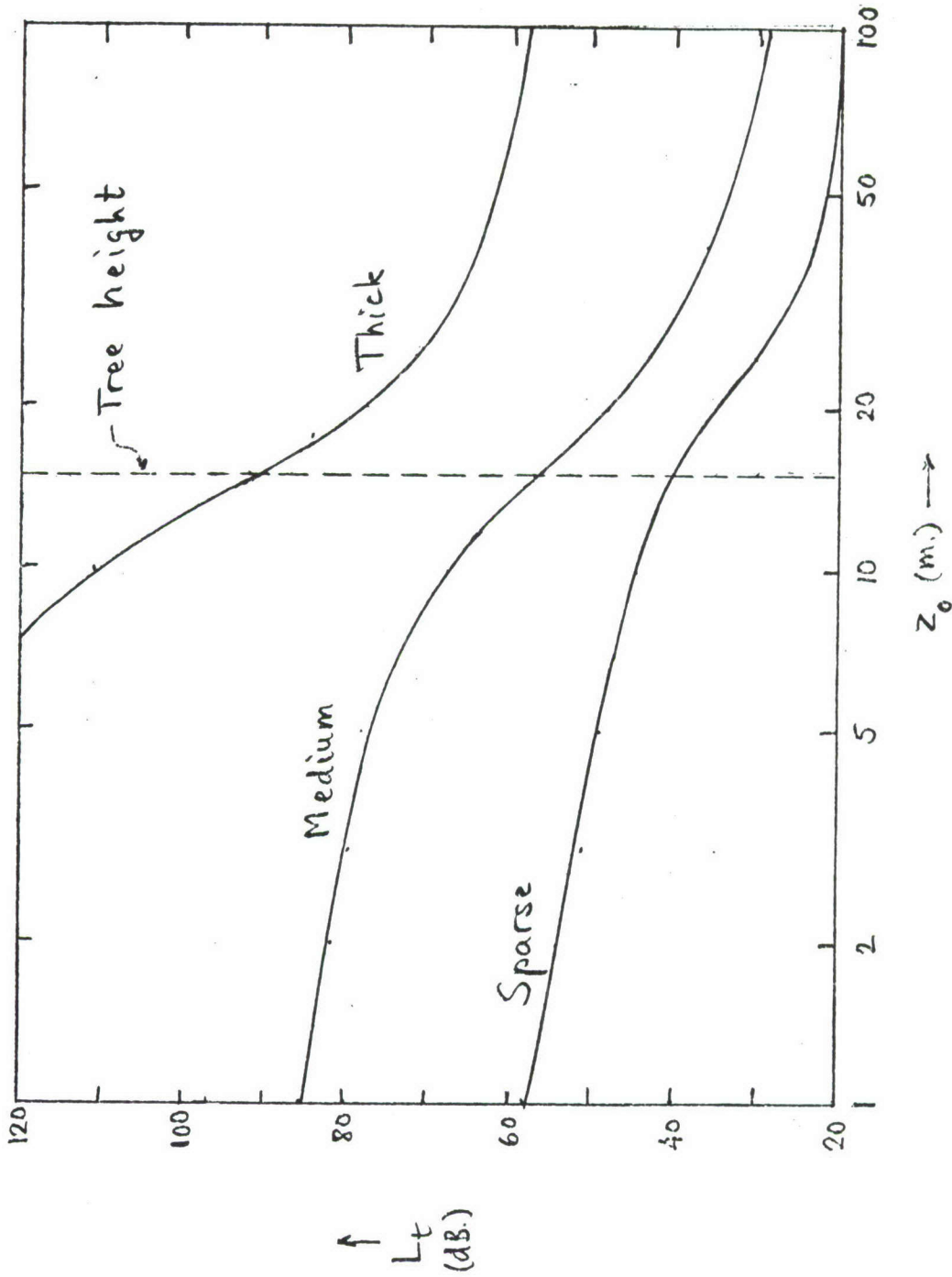


Fig. 12. Terrain loss L_t versus antenna height z_0 for various types of vegetation. Results shown are for a range $\rho = 500$ m.; average tree height $h = 15$ m. and target height $z' = 1$ m.

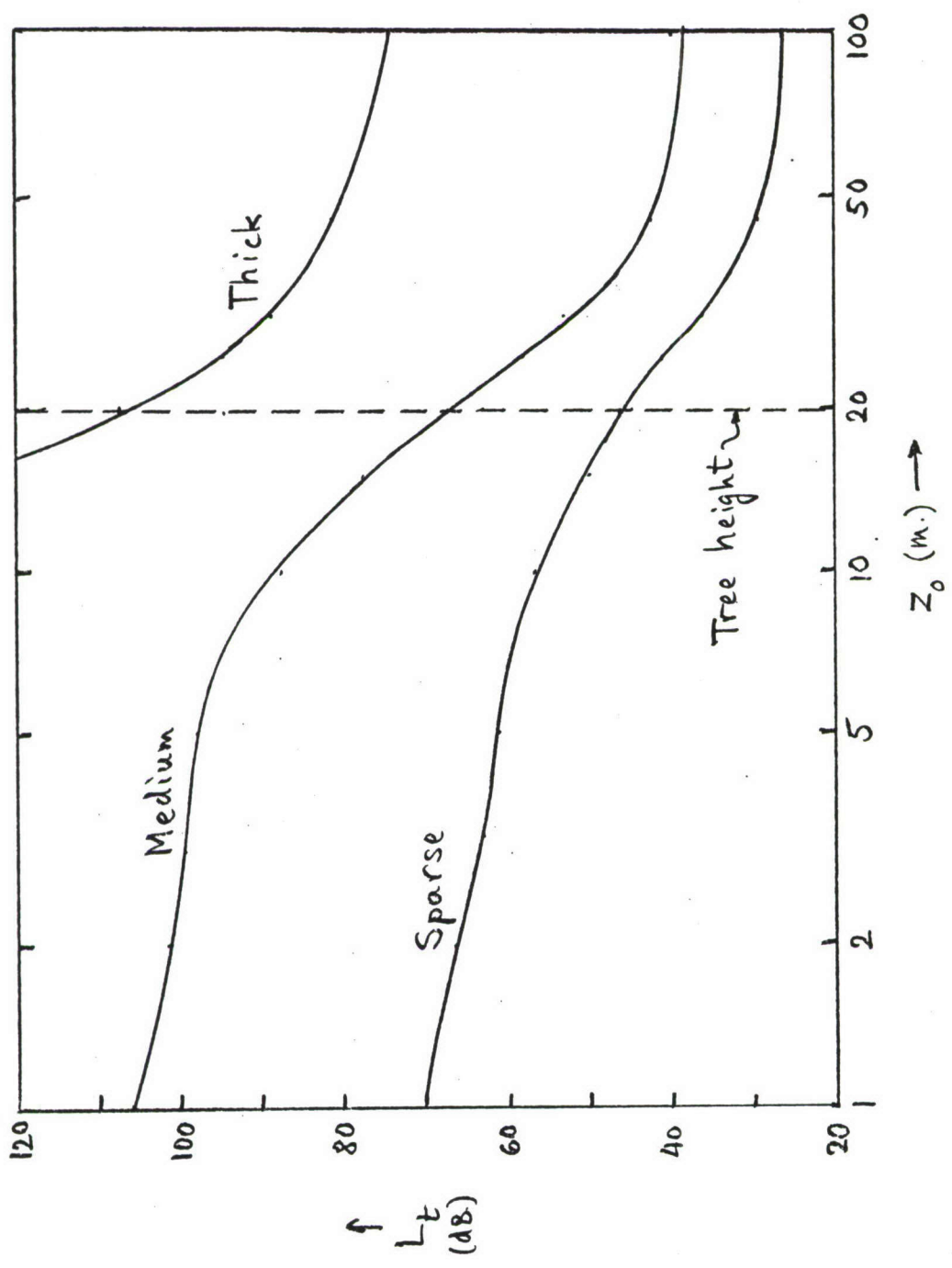


Fig. 13. Terrain loss L_t versus antenna height z_0 for various types of vegetation. Results shown are for a range $\rho = 500$ m., average tree height $h = 20$ m. and target height $z = 1$ m.

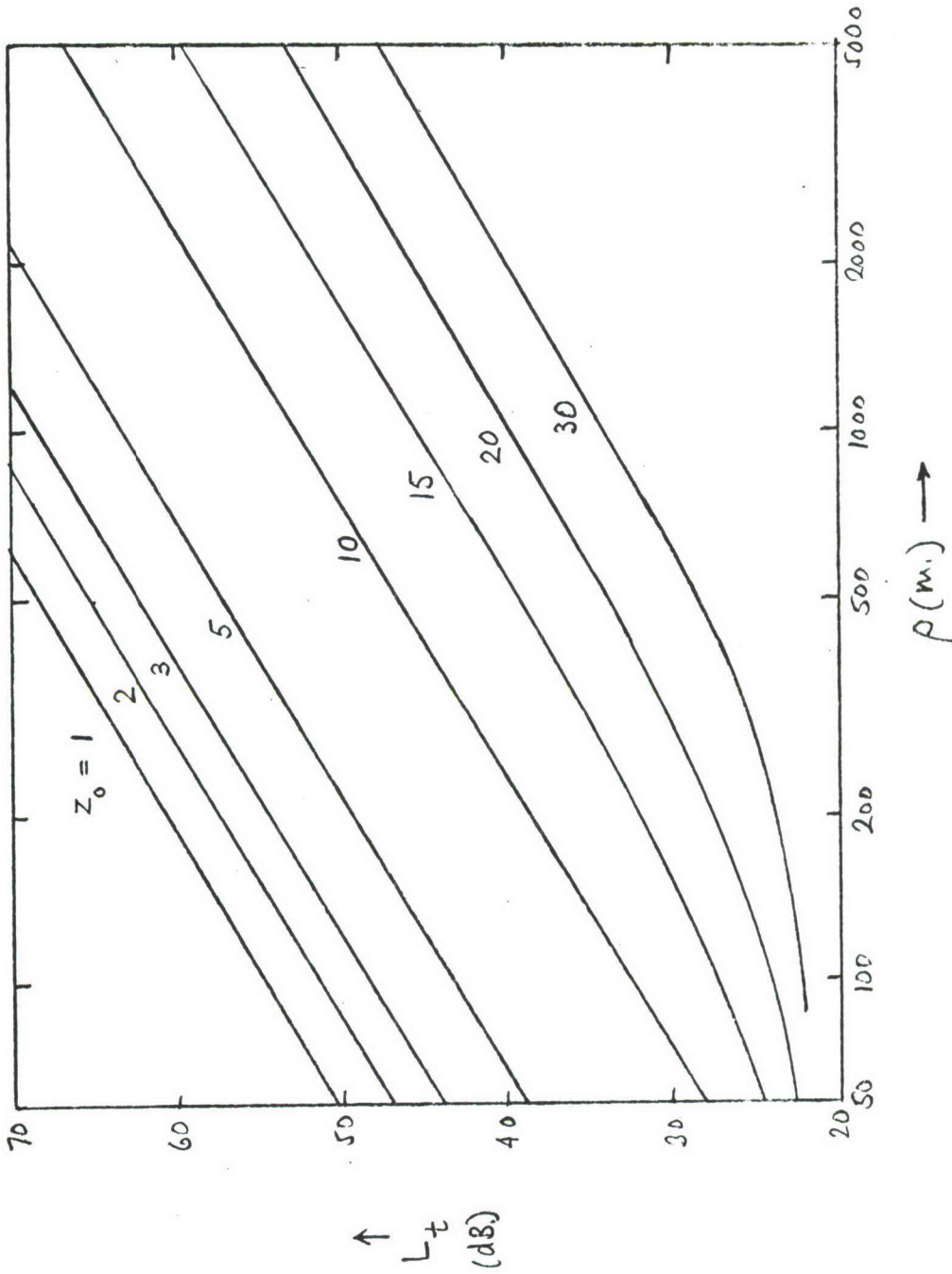


Fig. 14. Terrain loss L_t versus range ρ for various antenna heights z_0 .
 Results shown are for a forest with medium foliage and an average
 tree height $h = 10$ m.

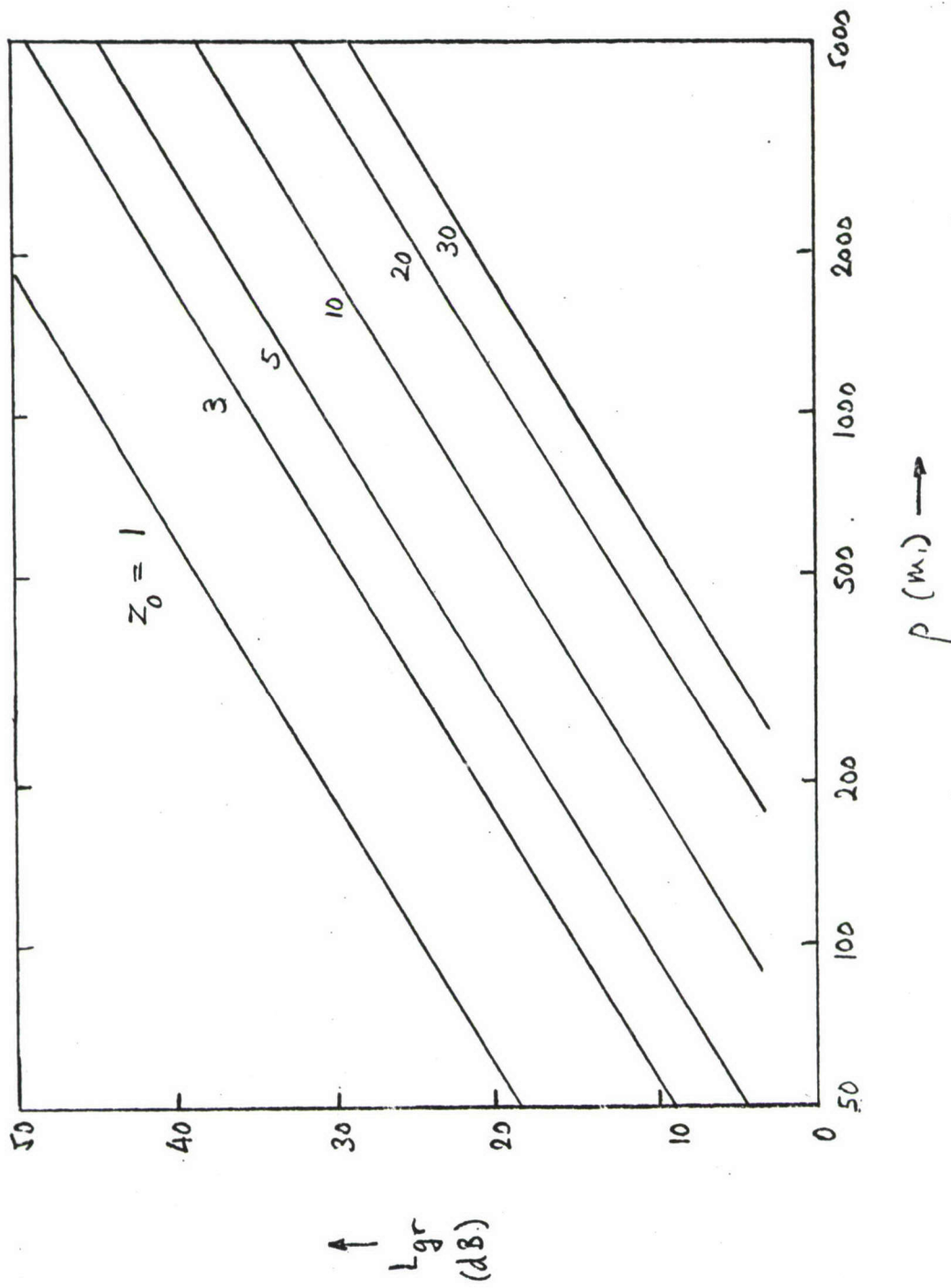


Fig. 15. Bare-ground loss L_{gr} versus range ρ for various antenna heights z_0 .

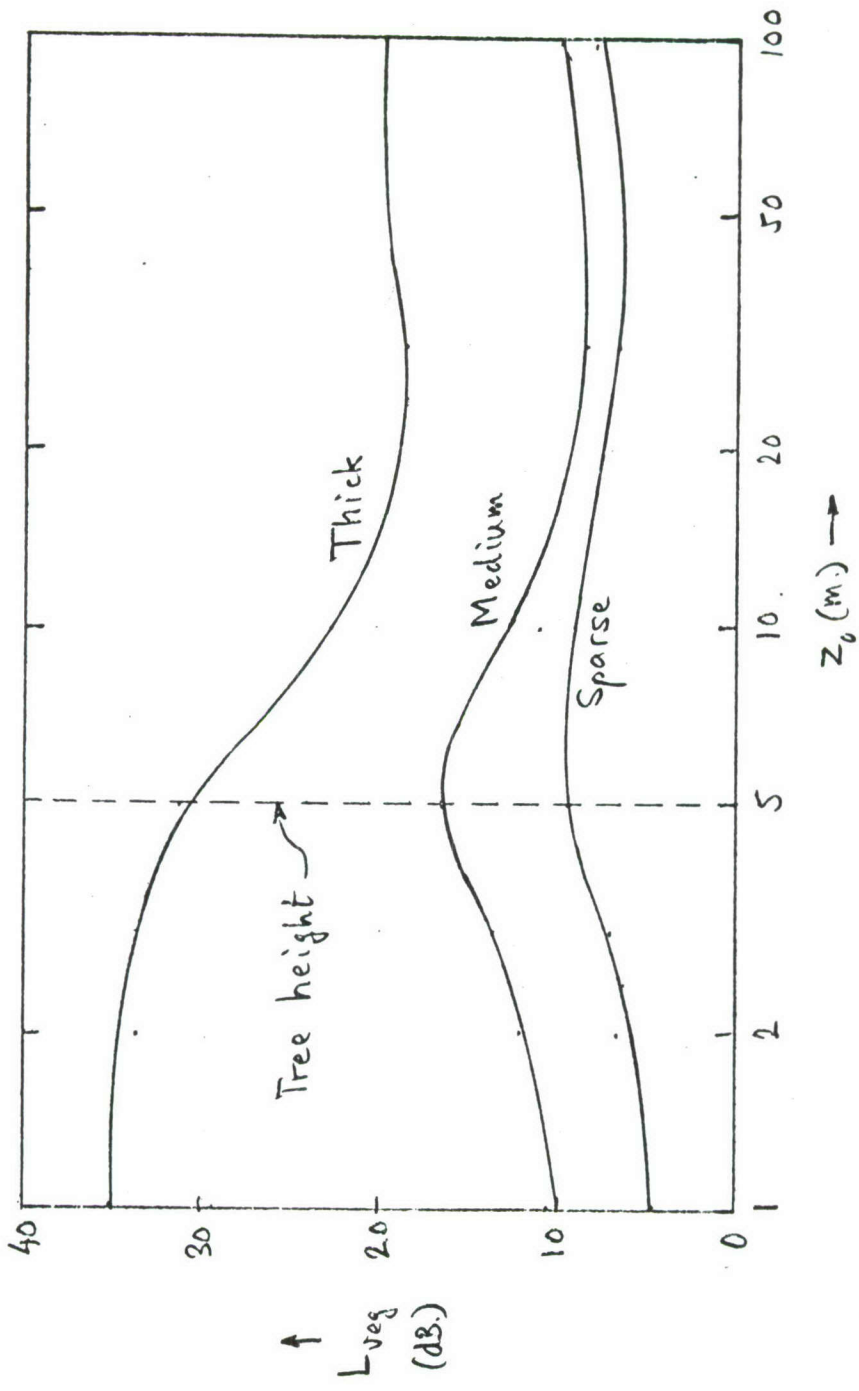


Fig. 16. Vegetation loss L_{veg} versus antenna height z_0 for various types of vegetation. Results shown are for an average tree height $h = 5$ m. and target height $z = 1$ m.; the range ρ may take on any value larger than $\rho_{min} \approx 3 z_0$.

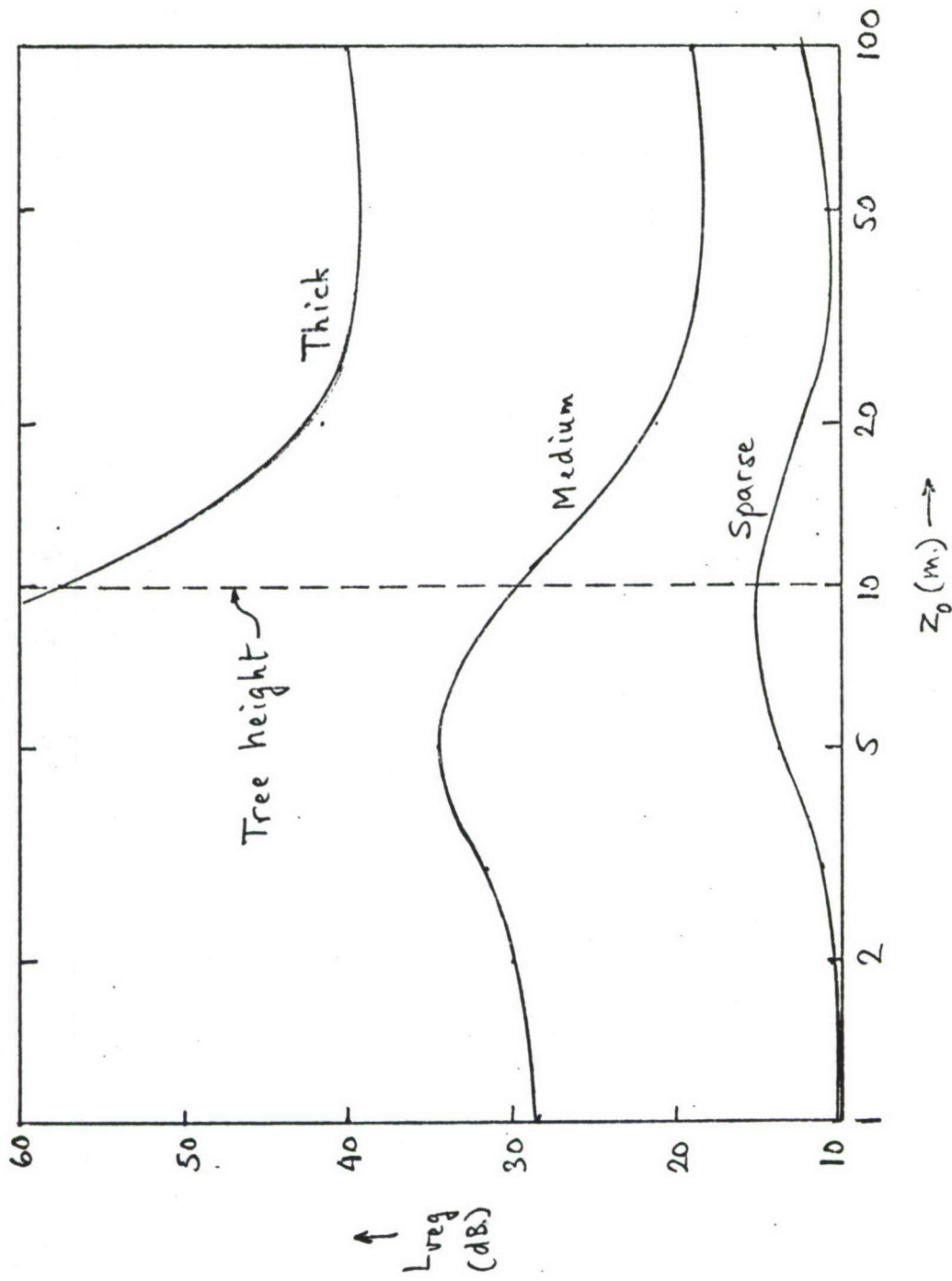


Fig. 17. Vegetation loss L_{veg} versus antenna height z_0 for various types of vegetation. Results shown are for an average tree height $h = 10$ m. and target height $z = 1$ m.; the range ρ may take on any value larger than $\rho_{min} \approx 3 z_0$.

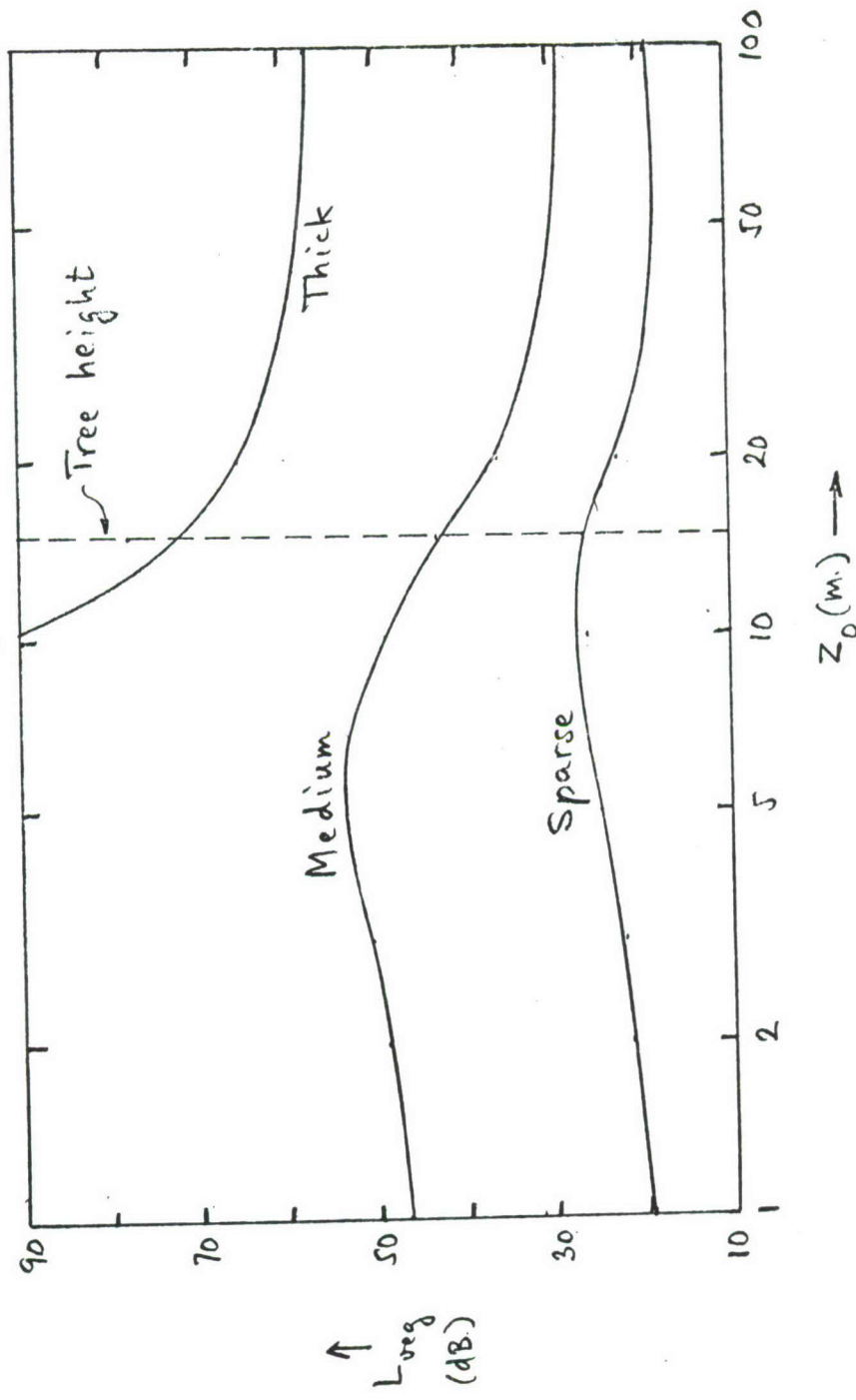


Fig. 18. Vegetation loss L_{veg} versus antenna height z_0 for various types of vegetation. Results shown are for an average tree height $h = 15$ m. and target height $z = 1$ m; the range ρ may take on any value larger than $\rho_{min} \approx 3 z_0$.

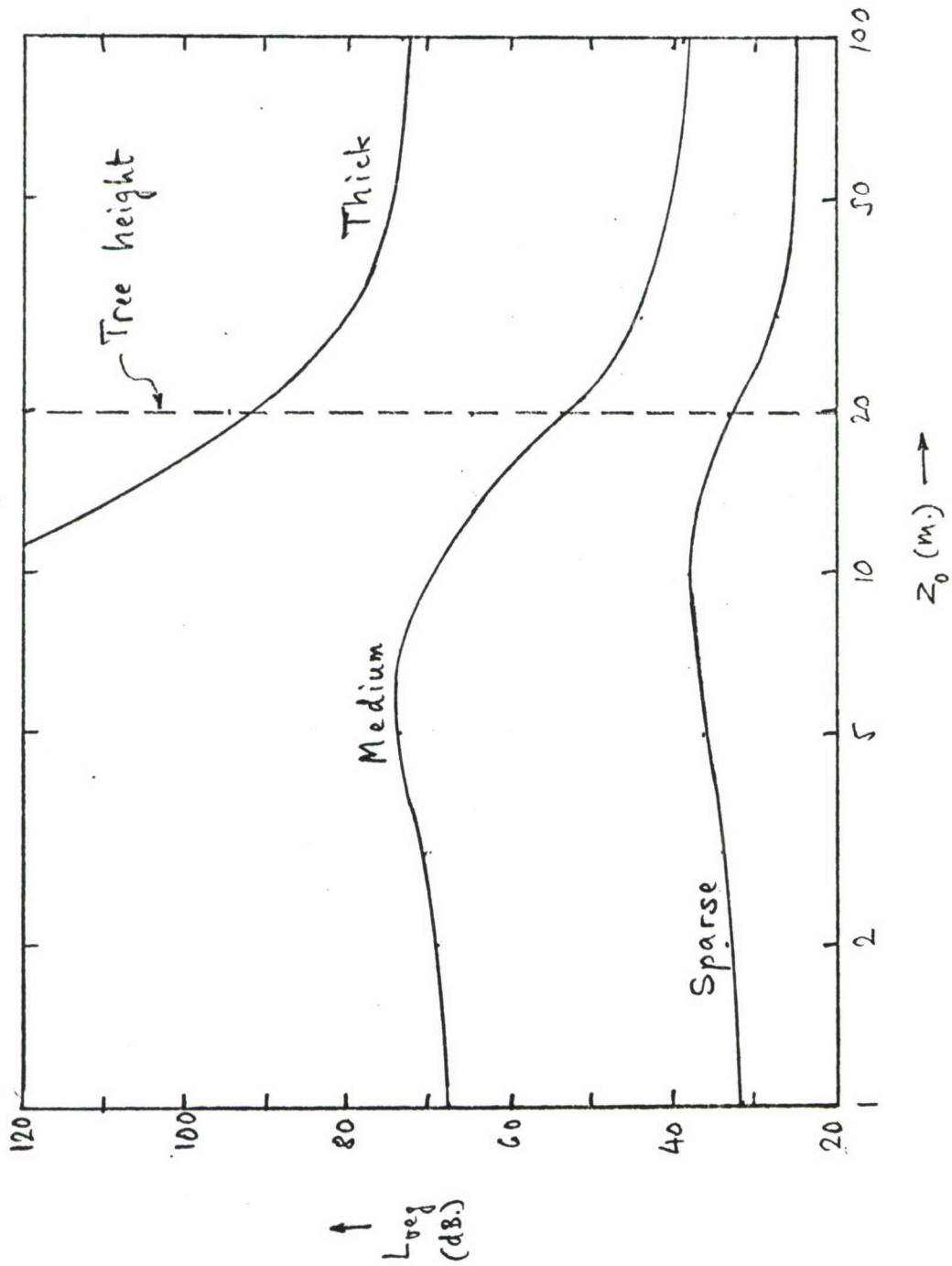


Fig. 19. Vegetation loss L_{veg} versus antenna height z_0 for various types of vegetation. Results shown are for an average tree height $h = 20$ m. and target height $z = 1$ m.; the range ρ may take on any value larger than $\rho_{min} \approx 3 z_0$.

DISTRIBUTION LIST

	<u>Copies</u>
Director Advanced Research Projects Agency Office, Director of Defense Research & Engineering ATTN: Assistant Director, Remote Area Conflict Washington, DC 20310	3
HQDA (DARD-DDS) WASH DC 20310	4
HQDA (DARD-ARZ-C) WASH DC 20310	1
HQDA (DAFD-ZB) WASH DC 20310	1
HQDA (FDCT) WASH DC 20310	2
Commanding General US Army Materiel Command ATTN: Director of Research and Laboratories Washington, DC 20315	1
Commanding General US Army Materiel Command ATTN: Director of Developments Washington, DC 20315	3
Commanding General US Army Materiel Command ATTN: AMCRD-PT Washington, DC 20310	1
US Army Combat Developments Command Liaison Officer Aberdeen Proving Ground, MD 21005	1
Commanding General US Army Combat Developments Command Combat Support Group Fort Belvoir, VA 22060	1
Commanding General US Army Test and Evaluation Command Aberdeen Proving Ground, MD 21005	1

	<u>Copies</u>
Commanding Officer US Army Combat Developments Command Institute of Strategic and Stability Operations Fort Bragg, NC 28307	1
Commanding General US Army John F. Kennedy Center for Special Warfare Fort Bragg, NC 28307	1
Commanding Officer US Army Concept Team in Vietnam APO San Francisco 96384	2
Senior Representative US Army Standardization Group, Australia c/o American Embassy Canberra, A.C.T., Australia	1
Director Air University Library ATTN: AUL3t-64-572 Maxwell Air Force Base, AL 36112	1
Director OSD/ARPA Research & Development Field Unit APO San Francisco 96243	1
Director OSD/ARPA Research & Development Center APO San Francisco 96346	1
Director of Defense Research & Engineering ATTN: Deputy Director for SEA Matters Department of Defense Washington, DC 20310	1
Battelle Memorial Institute Remote Area Conflict Information Center Columbus Laboratories 505 King Avenue Columbus, OH 43201	1
Defense Documentation Center (ASTIA) Cameron Station Alexandria, VA 22314	12

	<u>Copies</u>
Commanding Officer US Army Land Warfare Laboratory ATTN: RDLW-POA Aberdeen Proving Ground, MD 21005	4
Commanding Officer US Army Edgewood Arsenal ATTN: SMJEA-TS-L Edgewood Arsenal, MD 21010	1
USALWL Liaison Officer US Army Concept Team in Vietnam APO San Francisco 96384	1
HQDA (DAMI-ZD) WASH DC 20310	1
US Marine Corps Liaison Officer Aberdeen Proving Ground, MD 21005	1
HQDA (DAMO-PLW) WASH DC 20310	1
HQDA (DAMO-IAM) WASH DC 20310	1

DOCUMENT CONTROL DATA - R & D

(Security classification of title, body of abstract and indexing annotation must be entered when the overall report is classified)

1. ORIGINATING ACTIVITY (Corporate author) T. Tamir, Ph. D., Consultant to USALWL 981 East Lawn Drive Teaneck, N.J. 07666		2a. REPORT SECURITY CLASSIFICATION Unclassified	
		2b. GROUP	
3. REPORT TITLE Effect of a Forest Environment on the Performance of Doppler Radar Systems			
4. DESCRIPTIVE NOTES (Type of report and inclusive dates) Interim Report			
5. AUTHOR(S) (First name, middle initial, last name) T. Tamir, Ph.D.			
6. REPORT DATE 10 Nov 71		7a. TOTAL NO. OF PAGES 47	7b. NO. OF REFS 7
8a. CONTRACT OR GRANT NO. DA-31-124-AROD 120		9a. ORIGINATOR'S REPORT NUMBER(S)	
b. PROJECT NO. LWL Task 05-P-70			
c.		9b. OTHER REPORT NO(S) (Any other numbers that may be assigned this report)	
d.			
10. DISTRIBUTION STATEMENT Distribution of this document is unlimited			
11. SUPPLEMENTARY NOTES		12. SPONSORING MILITARY ACTIVITY U. S. Army Land Warfare Laboratory Aberdeen Proving Ground, Md. 21005	
13. ABSTRACT The aim of this report is to examine the effect of a forest environment on the performance of a remote sensing system that detects the Doppler-shifted signal scattered by moving objects. For this purpose, the influence of the terrain on the radar equation is determined by estimating the additional path loss due to the presence of dissipative media between the transmitter antenna and the moving scatterer. For most situations of practical importance, it is shown that the additional path loss can be expressed in terms of a terrain factor, which accounts for the presence of both the foliage and the ground. This terrain loss is evaluated for the case of a moving target located in the vegetation, and for a transmitter antenna that may be placed either inside the vegetation or above the tree tops. The calculated results are given for a wide range of distances between the antenna and the target, for various antenna heights and for different types of wooded areas.			

KEY WORDS	LINK A		LINK B		LINK C	
	ROLE	WT	ROLE	WT	ROLE	WT
Effect of vegetation on doppler radar systems Two way path loss in vegetation						